

NBS REPORT

8819

CRYOGENIC PROPELLANT VENTING UNDER LOW PRESSURE
CONDITIONS

Final Report under Government Order H-42001,

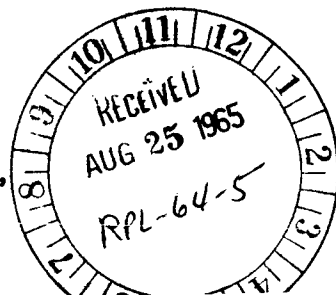
NASA Purchase Request TP3-85174

Prepared for George C. Marshall Space Flight Center,
N. A. S. A., Huntsville, Alabama

June 17, 1965

by

M. C. Jones, T. T. Nagamoto, J. A. Brennan,
Patricia J. Giarratano, and R. V. Smith



GPO PRICE \$ _____

CFSTI PRICE(S) \$ _____

N65-32046

(ACCESSION NUMBER)

(THRU)

46

1

(PAGES)

(CODE)

CR 64542

33

(NASA CR OR TMX OR AD NUMBER)

(CATEGORY)

Hard copy (HC) 2.00

Microfiche (MF) .50

FACILITY FORM 602

ff 653 July 65

Cryogenics Division

INSTITUTE FOR MATERIALS RESEARCH

U. S. DEPARTMENT OF COMMERCE

NATIONAL BUREAU OF STANDARDS

BOULDER LABORATORIES

Boulder, Colorado

THE NATIONAL BUREAU OF STANDARDS

The National Bureau of Standards is a principal focal point in the Federal Government for assuring maximum application of the physical and engineering sciences to the advancement of technology in industry and commerce. Its responsibilities include development and maintenance of the national standards of measurement, and the provisions of means for making measurements consistent with those standards; determination of physical constants and properties of materials; development of methods for testing materials, mechanisms, and structures, and making such tests as may be necessary, particularly for government agencies; cooperation in the establishment of standard practices for incorporation in codes and specifications; advisory service to government agencies on scientific and technical problems; invention and development of devices to serve special needs of the Government; assistance to industry, business, and consumers in the development and acceptance of commercial standards and simplified trade practice recommendations; administration of programs in cooperation with United States business groups and standards organizations for the development of international standards of practice; and maintenance of a clearinghouse for the collection and dissemination of scientific, technical, and engineering information. The scope of the Bureau's activities is suggested in the following listing of its four Institutes and their organizational units.

Institute for Basic Standards. Applied Mathematics. Electricity. Metrology. Mechanics. Heat. Atomic Physics. Physical Chemistry. Laboratory Astrophysics.* Radiation Physics. Radio Standards Laboratory.* Radio Standards Physics; Radio Standards Engineering. Office of Standard Reference Data.

Institute for Materials Research. Analytical Chemistry. Polymers. Metallurgy. Inorganic Materials. Reactor Radiations. Cryogenics.* Materials Evaluation Laboratory. Office of Standard Reference Materials.

Institute for Applied Technology. Building Research. Information Technology. Performance Test Development. Electronic Instrumentation. Textile and Apparel Technology Center. Technical Analysis. Office of Weights and Measures. Office of Engineering Standards. Office of Invention and Innovation. Office of Technical Resources. Clearinghouse for Federal Scientific and Technical Information.**

Central Radio Propagation Laboratory.* Ionospheric Telecommunications. Tropospheric Telecommunications. Space Environment Forecasting. Aeronomy.

* Located at Boulder, Colorado 80301.

** Located at 5285 Port Royal Road, Springfield, Virginia 22171.

**CASE FILE
COPY**

NATIONAL BUREAU OF STANDARDS REPORT

NBS PROJECT

31507-12-3150472

June 17, 1965

NBS REPORT

8819

CRYOGENIC PROPELLANT VENTING UNDER LOW PRESSURE CONDITIONS

Final Report under Government Order H-42001,
NASA Purchase Request TP3-85174
Prepared for George C. Marshall Space Flight Center,
N. A. S. A., Huntsville, Alabama

June 17, 1965

by

M. C. Jones, T. T. Nagamoto, J. A. Brennan,
Patricia J. Giarratano, and R. V. Smith

IMPORTANT NOTICE

NATIONAL BUREAU OF STANDARDS REPORTS are usually preliminary or progress accounting documents intended for use within the Government. Before material in the reports is formally published it is subjected to additional evaluation and review. For this reason, the publication, reprinting, reproduction, or open-literature listing of this Report, either in whole or in part, is not authorized unless permission is obtained in writing from the Office of the Director, National Bureau of Standards, Washington, D.C. 20234. Such permission is not needed, however, by the Government agency for which the Report has been specifically prepared if that agency wishes to reproduce additional copies for its own use.



U.S. DEPARTMENT OF COMMERCE
NATIONAL BUREAU OF STANDARDS

TABLE OF CONTENTS

	PAGE
ABSTRACT -----	1
1. INTRODUCTION -----	1
2. EXPERIMENTAL EQUIPMENT AND PROCEDURE	2
2.1. Experimental System -----	2
2.2. Test Sections -----	3
2.3. Instrumentation -----	4
2.4. Experimental Procedure -----	6
2.5. Calibrations -----	7
3. RESULTS -----	8
4. DISCUSSION OF RESULTS -----	12
4.1. Heat Transfer Mechanism -----	12
4.2. Design Considerations -----	14
5. NOMENCLATURE -----	16
6. REFERENCES -----	18
7. APPENDIX -----	20
Table 1 -----	20
Table 2 -----	32
FIGURES 1 through 10 -----	33

CRYOGENIC PROPELLANT VENTING UNDER LOW PRESSURE
CONDITIONS

M. C. Jones, T. T. Nagamoto, J. A. Brennan,
Patricia J. Giarratano, and R. V. Smith

Heat transfer coefficients have been measured to two-phase, single component, solid-vapor mixtures flowing through a short vertical tube. The two-phase mixtures were produced by venting liquids parahydrogen and nitrogen to pressures of from 4 to 17.5 mm Hg. At sufficiently high heat flux the mixtures have been found to flow freely through the tube with no tendency for solid to build up in the tube.

32046

Author

1. INTRODUCTION

The study described in this report was prompted by interest in the venting of cryogenic liquids to a low pressure ($\sim 10^{-6}$ mm Hg) space environment. It is hoped, however, that the information presented will be of value to the technology of handling solidified gases in general.

Liquids para-hydrogen and nitrogen at atmospheric pressure or above were flashed through an orifice down to a pressure of a few millimeters of mercury. Since these low pressures were below the respective triple points (53 mm Hg and 94 mm Hg), the emerging jet broke up into a stream of solid particles suspended in vapor. The particular properties of such a stream investigated in this study were its ability to

flow through a short length of vertical tubing and its heat transfer characteristics.

Early experiments conducted with a glass tube showed that flow of the mixture occurred only for a short period. Thereafter, solid built up on the wall, particularly adjacent to the orifice, and flow became intermittent, being obstructed by large agglomerations of solid. In some cases, the tube became completely blocked for several minutes with pressure above the blockage equilibrating with that upstream of the orifice and, consequently, liquid filling the tube above the blockage. This is illustrated in fig. 1 where high heat flux corresponds to initial behavior.

The fact that flow through the tube was possible initially, when the tube was warm, led to the conclusion that flow was essentially governed by heat transfer to the stream; it appeared impossible for solid to adhere to a warm tube, and one might hypothesize that this was due to the sublimation of particles as they approached the warm wall.

The experiments described below were carried out with a heated brass tube equipped with thermocouples and pressure taps so that heat transfer and flow could be studied under conditions of steady heat input.

In view of the exploratory nature of these experiments, the results are regarded as preliminary, and it is hoped to complete more controlled measurements in the future.

2. EXPERIMENTAL EQUIPMENT AND PROCEDURE

2.1. Experimental System

The experimental system is shown schematically in fig. 2. A large vacuum insulated dewar, A, was constructed, the inner wall of

which could be precooled by passing liquid nitrogen through the panels B₁, B₂, and B₃. A coarse vacuum (not less than 2 mm Hg) could be maintained inside the dewar by pumping through the 6" line G with either one, two, or three reciprocating vacuum pumps C₁, C₂, and C₃, each having a capacity of 650 CFM at 10 mm Hg. The dewar was fitted with a 6" diameter, double-glass, evacuated window (F) for visual observation.

The test liquid filled the storage vessel D, of 9 liters capacity, which could be pressurized or run at essentially atmospheric pressure with boil-off passing through wet test meter E, via heat exchanger H consisting of a copper coil in a tub of water.

At the bottom of D was situated a 3/4" diameter neck accommodating at its lower end an orifice drilled in a 0.016" thick, circular, stainless steel plate. Flow rate was varied by interchanging plates with different sized orifices or by varying the pressure in vessel D. Four orifices were used in these experiments with diameters respectively 0.144, 0.105, 0.089, and 0.059 cm.

2.2. Test Sections

Interchangeable test sections may be slipped over the orifice plate neck and soft soldered to the base of the vessel D. In the initial experiments, a glass test section was attached by a "Kovar" glass-to-metal seal and for the later experiments, where the heat transfer measurements described in this report were made, a brass tube equipped with a heater was used. In each case, the test section was in essence a straight tube of a little over one foot in length and nominally 1" diameter, which could be viewed through the window F. Each was fitted with four equally spaced pressure taps and a corresponding thermocouple.

The brass test section is shown in detail in fig. 3. It was attached

to the vessel D via a thin wall (0.020"), stainless-steel transition to limit heat conduction to and from the vessel. The four copper-constantan thermocouples were laid in helical grooves, 0.020" wide and 0.015" deep at 3" spacing, machined in the tube wall which, having 1/32" wall thickness, left approximately 0.016" thickness of brass separating the junctions from the flow stream. Tempering of the thermocouples was obtained for three turns in the helical grooves followed by a length along the outer tube wall to the top of the tube. The thermocouple wire, both in the grooves and along the tube, was cemented to the tube with varnish. Finally, in order to enclose the junctions in an isothermal region as nearly as possible, thin strips of brass were soft soldered over the grooves.

The application of heat through the brass tube wall was required to be done in such a way that no temperature gradients were induced in the thermocouple wires. This was done by covering the tube and thermocouple leads with a layer of "Fiberglas" paper which, when attached, was soaked in varnish. The heater was wound noninductively, uniformly, and closely over this from 26-gauge, double-glass-covered "Advance" wire and again soaked in varnish.

It would have been desirable then to enclose the whole tube in a vacuum insulation with a radiation shield. However, the exploratory nature of the experiments led us to prefer a simpler approach where the insulation was obtained by six further layers of "Fiberglas" paper soaked on with varnish followed by alternate layers of aluminum foil and compressed glass wool, giving a total insulation thickness of about 1 1/2".

2.3. Instrumentation

Power from a 3-phase, 208-volt source was fed through a 3-phase auto transformer and full-wave, bridge rectifier circuit to the tube

heater and measured by a moving coil ammeter and voltmeter. Accuracy of this measurement is considered to be within 5%.

Thermocouple emf's were referenced to the liquid in the vessel D and measured by a potentiometer, the unbalance being fed to a D. C. amplifier and displayed on a recording oscillograph. In this way, the emf's could be measured to within $2 \mu\text{V}$ although fluctuations in the emf's made this accuracy somewhat superfluous. The temperature of the liquid in the storage vessel D was measured by a platinum resistance thermometer. The potential drop was measured on the same potentiometer as the thermocouple emf's while the thermometer current was measured with a second potentiometer as the potential drop across a standard 1 ohm resistor. The measured liquid temperature was accurate to 0.05°K at liquid hydrogen temperature and considerably better at liquid nitrogen temperature.

Pressures along the test section and in the dewar were measured in turn with a McLeod gauge. The readings obtained were reproducible to 0.5 mm Hg. In the calculation of heat transfer coefficients, the bulk stream temperatures were assumed to be the saturation temperatures corresponding to these pressures, since no simple method could be devised for a direct temperature measurement. Hence, within the limitations of this assumption, the 0.5 mm Hg corresponded to a worst uncertainty of about 0.3°K for nitrogen (5 mm Hg, 51.6°K) and 0.1°K for hydrogen (5 mm Hg, 10.9°K).

The rate of flow of liquid through the orifice was determined by a continuous record on the oscillograph of liquid level in the storage vessel. The signal for this was derived from a capacitance liquid-level gauge balanced across an A. C. bridge circuit against a standard capacitor. The capacitance gauge itself consisted of two concentric tubes

(3/4" O.D. and 7/8" O.D. x 11 3/4") standing in the storage vessel and fitted with drainage holes. Thus, the capacitance, depending on the depth of liquid in the vessel and the difference in the dielectric constants of the liquid and vapor, was linear with liquid depth. Prior to assembly, the storage vessel capacity had been calibrated against depth and was also found to be linear. From this calibration the total volume between top and bottom of the capacitance gauge could also be obtained (8,740 ml).

To correct flow rates obtained from the rates of fall of liquid level for boil-off from the storage vessel, the boil-off gas was passed through the heat exchanger, H, and then through the wet test meter, E.

2.4. Experimental Procedure

For both hydrogen and nitrogen runs, the inner wall of the dewar was first precooled with liquid nitrogen and the dewar evacuated, using one of the pumps, C. The storage vessel D was then filled with the test liquid and extra pumps were cut in, as necessary, to maintain the vacuum between 4 and 5 mm Hg. In some cases, however, where high power was applied to the test section, dewar pressure ran as high as 17.5 mm Hg. Liquid from D discharged into the dewar forming solid, which collected in the bottom of the dewar, and vapor which was pumped off. The storage vessel was allowed to empty completely once before any measurements were taken in order to achieve cooldown of the inner wall of the dewar and all supports leading to the vessel itself. At this point too, the position on the oscillograph chart, corresponding to no liquid in the capacitance level gauge, was noted. Completion of the second filling of the storage vessel was indicated by a leveling off of the liquid level chart trace, and this was taken to indicate that the capacitance gauge was full.

The system was now ready for a heat transfer measurement.

Power was applied to the test section until the thermocouple emf's indicated the required temperature. It was then adjusted until a power level was found at which temperatures stabilized and, after several minutes of such steady operation, the emf's were recorded in turn, together with the potential drop across the platinum resistance thermometer. At this time also the McLeod gauge was read at each station. Normally, the highest power level to be run was applied first and successively lower levels applied until either the tube began to plug with solid or the power was considered to be at the lower limit for accurate measurement.

With the larger orifices and, consequently, higher discharge rates solid tended to pile up in the bottom of the dewar to such a height that free discharge from the tube was impeded. In these cases, it was found possible to maintain unimpeded operation by operating a wiper arm, which reached down into the dewar and with which the solid could be pushed clear. This circumstance set an upper limit to orifice size used. A lower limit was set by two factors. First, since boil-off was independent of orifice size, the boil-off correction to flow rate became proportionately larger for the small orifices. Secondly, the discharge through a small orifice was found to be quite variable and steadily decreased during the course of a day's run. It seems likely that solid impurities may have built up in the small orifices.

2.5. Calibrations

The wall thermocouples were calibrated by a single temperature check in which the brass test section was made into an ice bath by plugging the lower end, and the cold junction was immersed in liquid nitrogen. A single factor for each thermocouple was then applied to the standard copper-constantan tables of Powell, Bunch, and Corruccini [1] to give the correct value of emf at this point.

A second calibration required was for the heat loss through the insulation of the brass test section. This was done at room temperature by inserting glass wool into the tube to eliminate convection and by plugging both ends of the tube. In this way all heat applied had to leave through the insulation at steady state. The wall temperatures for a single low power input were recorded at steady state, and it was assumed that the heat loss was radial through the insulation and was proportional to the difference between the wall temperatures and the outside temperature of the insulation. Since it was recognized that the thermal conductivity of the insulation would decrease with temperature the determination was performed again with the test section cooled to liquid nitrogen temperature. The constant of proportionality was approximately halved in this case. The latter value was used for all corrections to power since it represented a safe upper limit; the outside of the test section was always colder than liquid nitrogen during an experiment, being swept by vapor subliming from the solid in the bottom of the dewar.

3. Results

In order to analyze the results it was necessary to calculate the quality of the mixture at each station. Having calculated that the kinetic energy of the stream was negligible an energy balance could be applied as follows:

$$MH_L = Mx_n H_v + M(1 - x_n) H_S - qA_n .$$

Enthalpies below the triple point for para-hydrogen were obtained from Mullins, Ziegler, and Kirk [2], while those for nitrogen were calculated from the solid specific heat and heats of sublimation given by Ziegler and Mullins [3]. The computed solid enthalpies were found to be in agreement with the few points given by Din [4]. Liquid enthalpies

were obtained from Roder and Goodwin [5] and Strobridge [6], respectively, for para-hydrogen and nitrogen. With quality thus determined at each station a mean density and mean fluid velocity could be calculated.

In the calculation of such quantities as Reynolds no. $\frac{GD}{\mu_b}$, Prandtl no., $\frac{\mu_b C_p}{k_b}$ and Nusselt no. $\frac{h_{exp} D}{k_b}$ the transport properties

of the vapors were required. Viscosities at these low temperatures were obtained by extrapolation of the low pressure viscosities given by Johnson, ed. [7] using the Chapman-Enskog formula for monatomic gases. Thermal conductivities were computed from the Eucken equation using these viscosities and the specific heat derived from the enthalpies mentioned above.

The heat flux, q watts/cm², to the solid-vapor stream was calculated at each station from the power input and the heat leak, assumed to be radial, through the insulation. The temperature difference, $\Delta T^\circ K$, between the inside wall and the bulk stream was calculated from the measured outside wall temperature, corrected for temperature drop through the wall, and the solid-vapor saturation temperature corresponding to the pressures measured at each station. The experimental heat transfer coefficient, h_{exp} , is then $q/\Delta T$ for each station.

The uncertainty in heat flux measurement was about 5%. The percentage correction due to heat leak through the insulation was quite variable and was different for hydrogen and nitrogen. For hydrogen most corrections were less than 5%, but for a few points corrections as high as 16% were applied. For nitrogen the corresponding figures were 25% and 38%. Combined uncertainties in the measurement of temperature difference led to a worst uncertainty of 0.6°K for both hydrogen

and nitrogen.

Each orifice with each liquid gave a more or less constant Reynolds no. so that an experimental run can be defined by a Reynolds no. or range of Reynolds nos. The results for hydrogen at station 4 are shown in fig. 4 as a plot of q vs ΔT for all the Reynolds no. ranges measured. The corresponding results for nitrogen are shown in fig. 8. In fig. 5 the influence of position along the tube is illustrated by plotting q vs ΔT at each station for hydrogen in the Reynolds no. range 74,000 - 113,000. Complete tabular results are given in an appendix, table 1.

It was hoped that either from visual observations or by inspection of results that the regime of free flow through the tube could be delineated. Certainly, a lower heat flux limit exists as is evident from visual observations (see fig. 1) on the mixture discharging from the tube that, as power was reduced, a flaky or lumpy mixture replaced the homogeneous, powdery mixture. This eventually led to a blockage as for the unheated glass tube. Only for the largest orifice used (0.144 cm dia) was the lower limit indicated by pressure fluctuation and this for both hydrogen and nitrogen. This is indicated in figs. 4 and 8 by the heavy dashed line. Otherwise, the transition from a free flowing, homogeneous, powdery mixture to an extremely heterogeneous mixture was uneventful and could not even be seen in the graphs of q vs ΔT . It is noticeable, however, that in many cases the plot of q vs ΔT changes from a straight line at approximately 45° to a flatter line at low heat fluxes. Comment on the anomalous high heat flux at which this occurred in fig 4, Reynolds no. range 120,000 to 190,000 will be reserved to the Discussion, section 4.2. Apparently in other cases, particularly the lower Reynolds no. runs, a low enough heat flux was not applied. It should be stressed that this change of slope did not coincide with change in appearance of the discharging mixture; heterogeneous discharge was already present above

this point. It is felt that more work needs to be done on the question of the lower limit of free flow.

Further comments are necessary on the behavior of nitrogen. One striking difference between the two fluids was that, in general, nitrogen discharged in a heterogeneous manner with the temperature at station 1 always a little above the local saturation temperature, insensitive to variations in power input and very unsteady. In the case of hydrogen, homogeneous discharge could always be obtained at high enough power inputs, the temperature at station 1 responded to power variations and it was steady. With the smallest orifice used (0.059 cm dia) two different runs were obtained for nitrogen (see table 1, runs no. 9 and 10 and fig. 8). The first was normal for nitrogen (run no. 9, Reynolds no. range 20,000 - 26,000). In the second run (run no. 10, Reynolds no. range 4,000 - 19,000) the behavior was more typical of hydrogen in that it was found possible to run with station 1 at a higher temperature, steady, and with homogeneous discharge. Unfortunately, any effect the different flow pattern might have had on the q vs ΔT plot was obscured by the fact that in the second run the Reynolds no. decreased steadily during the run. The same dualistic behavior for nitrogen was obtained for a few high power inputs with the next smallest orifice (0.089 cm dia, run no. 8, Reynolds no. 47,000 - 53,000). However, in this case it was found impossible to complete a run of the second kind; the temperature of station 1 dropped to around the local saturation value quite abruptly below a certain power level.

Of some interest are the coefficients of discharge of the orifices presented in table 2. In general, these values are considerably below those reported by Brennan [8], although the orifice Reynolds nos. are comparable. The chief cause for the discrepancy is probably that in the present measurements the liquid upstream of the orifice was at its

saturation temperature, whereas Brennan's work was carried out with subcooled liquid. Saturated liquid may well cavitate inside the orifice. The very small discharge coefficients found for the 0.059 cm orifice were probably caused by solid blockage of the orifice because, as noted above, the discharge coefficient decreased during the course of a run.

4. Discussion of Results

4.1. Heat Transfer Mechanism

As can be seen from fig. 5 and as would be expected in an entrance region the heat transfer coefficient decreases with distance along the tube. It is convenient, in order to eliminate the effect of varying flow rate, to consider the ratio $\frac{h_{\text{exp}}}{h_{\text{calc}}}$, where h_{calc} is calculated from the Seider and Tate correlation:

$$\frac{h_{\text{calc}} D}{k_b} = 0.026 \left(\frac{DG_v}{\mu_b} \right)^{0.8} \left(\frac{C_p \mu_b}{k_b} \right)^{0.33} \left(\frac{\mu_b}{\mu_o} \right)^{0.14}$$

for vapor alone travelling at the same velocity as the mixture. Since h_{calc} is for a gas in a length of pipe far removed from the entrance, any variation of the ratio $\frac{h_{\text{exp}}}{h_{\text{calc}}}$ from 1.0 can be ascribed to either the presence of the second phase or to entrance effects. It is found that this ratio for a particular station (except at station 1 where there is excessive data scatter) correlates very well for hydrogen with the dimensionless group $\frac{q}{\rho_{vb} V \lambda}$ over the entire range of Reynolds nos. This group occurs in the forced convection boiling literature and has been called the boiling number. The two quantities are plotted in fig. 6 for each station. Also indicated on fig. 6 for stations 1, 2, and 3 is the boiling number for which the calculated quality, x , is 1.0 at each

station. It is significant that for station 4, where entrance effects would be almost completely absent in single phase flow, that $\frac{h_{exp}}{h_{calc}}$ approaches 1.0 as the boiling no. approaches its $x = 1.0$ value. For low values of boiling no. the value 2.0 is approached asymptotically.

Results for nitrogen did not correlate well when $\frac{h_{exp}}{h_{calc}}$ was plotted against boiling no. This may be seen from fig. 9 where for station 4 the hydrogen and nitrogen data are plotted together. In general the nitrogen data fall below hydrogen data, the one exception being for the nitrogen run (run no. 10 of table 1) with the 0.059 cm dia orifice in which experimental behavior was more like hydrogen as described in section 3 above. The generally different behavior of nitrogen does not, however, provide a conclusive explanation of the lack of correlation of the nitrogen data with the hydrogen data; some of the data points for the 0.089 cm dia orifice (run no. 8) also exhibited hydrogen-like behavior and yet fell below the hydrogen data. The apparent scatter of the nitrogen data may be due in part to error in the heat leak correction which is considered excessive for nitrogen and points to the inadequacy of the insulation provided.

Entrance effects may be illustrated by plotting the heat transfer coefficient ratio versus distance along the test section, represented dimensionlessly by $\frac{z}{D}$. This has been done in fig. 7 for hydrogen, which was cross-plotted from fig. 6. For comparison, the same ratio calculated by Sparrow, Hallman and Siegel [9] for single phase, fully developed turbulent flow is shown. Their results are for Reynolds nos. of 50,000 to 100,000 and a Prandtl no. of 0.7, while the experimental Reynolds no. range for the vapor alone travelling at the mean velocity of the mixture was 5,000 - 100,000 with a Prandtl no. of 0.69.

In the present two-phase case it is impossible to obtain a thermal

entrance region with a fully developed velocity profile existing over the entire region because in order to obtain flow of the solid-vapor mixture at all, heat must be applied at the tube inlet (orifice in this case). However, at station 4 the indications are that flow is fully developed since as quality approaches 1.0, h_{exp} approaches h_{calc} . It is then fairly certain that the presence of solid is alone responsible for the enhancement of h_{exp} at station 4 to the value of $2 h_{calc}$ at low boiling nos.

A plausible explanation of this enhancement can be found if it is supposed that vaporization of solid occurs only in the vicinity of the heated wall and that the latter then becomes blanketed by a film of vapor. This is illustrated in fig. 10. Whereas in the single-phase gas a temperature gradient exists across the whole tube radius, in the two-phase case, unless the vaporization process is very slow the temperature drop must be confined to the vapor film.

4.2. Design Considerations

The results of these experiments show that at sufficiently high heat fluxes through the tube wall a vapor-solid mixture can be effectively discharged through a short tube and, presumably, through other equipment with appropriate adjustments to the heat flux. Although a lower heat flux limit has not yet been established, it is safe to say from the data presented that free flow will be obtained at heat fluxes which lie on the upper, approximately 45° , straight line portion of the q vs ΔT curves. Furthermore, the higher the heat flux, the better.

In the course of these experiments it was discovered that the minimum heat flux required for free flow can be seriously affected by obstructions on the tube wall. In fig. 4, (Reynolds no. range 120,000 to 190,000) the unexpectedly high heat flux required to remain on the 45° straight line portion of the curve can be explained by the presence in

this run of a small projection into the tube at station 4 in the form of about 1/16" of 18 gauge bare copper wire. This was the tip of a probe which was inserted in order to detect, if possible, any electrostatic charges carried by the solid. The results of the test were negative, but it was found later that for the low temperature points station 4 was colder than 3. It is therefore suspected that solid built up at the tube wall in front of this projection which would not normally have happened until lower heat fluxes. This point is discussed here to serve as a caution to designers to avoid such obstacles in the flow path. The tube used here was of commercial grade, but the inside wall was lightly polished and was quite smooth. It is conceivable that excessive roughness might produce the same result and should therefore be avoided.

These results are for essentially parallel flow. In real equipment this is not likely to be the case with elbows and constrictions more probable. Future work will include the establishment of free-flow heat fluxes for direct impingement or stagnation flow. Such a case, it is felt, should represent the worst condition for the build-up of solid on a wall.

5. Nomenclature

A_n	Inside surface area of test section up to n^{th} station.	cm^2
Bo.	Boiling no., $= \frac{q}{\rho_{vb} V \lambda} = \frac{q}{G \lambda} \frac{\bar{\rho}}{\rho_{vb}}$,	
C_{pb}	Constant pressure specific heat of vapor at bulk conditions.	$\text{J/g} \cdot ^\circ\text{K}$
D	Inside diameter of test section	cm
G	Mass velocity in test section	$\text{g/cm}^2 \cdot \text{sec}$
H_L	Enthalpy of liquid in vessel D	J/g
H_s	Enthalpy of saturated solid	J/g
H_v	Enthalpy of saturated vapor	J/g
h_{calc}	Heat transfer coefficient calculated from Seider and Tate correlation for vapor travelling at velocity V	$\text{W/cm}^2 \cdot ^\circ\text{K}$
h_{exp}	Experimental heat transfer coefficient, $q/\Delta T$	$\text{W/cm}^2 \cdot ^\circ\text{K}$
k_b	Thermal conductivity of vapor at bulk conditions	$\text{W/cm} \cdot ^\circ\text{K}$
M	Mass flow rate	g/sec
Nu	Nusselt no., $\frac{h_{\text{exp}} D}{k_b}$	
q	Heat flux at test section wall	W/cm^2
Pr.	Prandtl no., $\frac{\mu_b C_{pb}}{k_b}$	
Re.	Reynolds no., $\frac{GD}{\mu_b}$	

T	Temperature	°K
ΔT	Inside wall temperature - local saturation temperature	°K
V	Mean velocity in test section $\frac{G}{\rho}$	cm/sec
x_n	Quality (g vapor/g mixture) at n th station	
z	Axial distance along test section measured from top of heated portion	cm
λ	Latent heat of sublimation	J/g
μ_b	Viscosity of vapor at bulk conditions	g/sec-cm
μ_w	Viscosity of vapor at wall temperature	g/sec-cm
$\bar{\rho}$	Mean density in test section	g/cc
ρ_{vb}	Density of vapor at bulk conditions	\bar{g}/cc
ρ_s	Density of solid	g/cc

Note: Bulk conditions in this report are taken to be local pressure and corresponding saturation temperature.

6. References

- [1] R. L. Powell, M. D. Bunch, and R. J. Corruccini, "Low Temperature Thermocouples - 1. Gold-Cobalt or Constantan versus Copper or 'Normal Silver'." *Cryogenics* 1, 139 (1961).
- [2] J. C. Mullins, W. T. Ziegler, and B. S. Kirk, "The Thermodynamic Properties of Parahydrogen from 1° to 22°K." Technical Report No. 1, Project No. A-593, November 1, 1961, Engineering Experiment Station of the Georgia Institute of Technology, Atlanta, Georgia.
- [3] W. T. Ziegler and J. C. Mullins, "Calculation of the Vapor Pressure and Heats of Vaporization and Sublimation of Liquids and Solids, Especially Below One Atmosphere. IV. Nitrogen and Fluorine." Technical Report No. 1, Project No. A-663, April 15, 1963, Engineering Experiment Station of the Georgia Institute of Technology, Atlanta, Georgia.
- [4] F. Din, "Thermodynamic Functions of Gases." Volume 3. (Butterworth and Co., Ltd., London, 1961).
- [5] H. M. Roder and R. D. Goodwin, "Provisional Thermodynamic Functions for Para-Hydrogen." N.B.S. Technical Note 130, December 1961, National Bureau of Standards, Boulder, Colorado.
- [6] T. R. Strobridge, "The Thermodynamic Properties of Nitrogen from 64 to 300°K between 0.1 and 200 Atmospheres." N.B.S. Technical Note 129, January 1962, National Bureau of Standards, Boulder, Colorado.

- [7] V. J. Johnson (editor) (1960), "A Compendium of the Properties of Materials at Low Temperature. Part I, Properties of Fluids," Wright Air Development Division Technical Report 60-56, National Bureau of Standards, Cryogenic Engineering Laboratory, Boulder, Colorado.
- [8] J. A. Brennan, "A Preliminary Study of the Orifice Flow Characteristics of Liquid Nitrogen and Liquid Hydrogen Discharging into a Vacuum." *Advances in Cryogenic Engineering* 9, 292 (Plenum Press, New York, N. Y., 1964).
- [9] E. M. Sparrow, T. M. Hallman, and R. Siegel, "Turbulent Heat Transfer in the Thermal Entrance Region of a Pipe with Uniform Heat Flux." *Appl. Sci. Res. Section A*, 7, 37 (1957).

7. Appendix

Table 1. Experimental Results

Explanation of Table

Column 1. "Run." Each run is characterized by an orifice diameter, a range of Reynolds nos. and the fluid used.

2. "Discharge Press. (mm Hg.)" Pressure inside dewar A into which the test section discharges.

3. " G ($\text{g}/\text{cm}^2\text{-sec}$)" Mass velocity inside test section.

4. "Sta." Station number along test section (see fig. 3).

5. " q (W/cm^2)." Heat flux corrected for heat loss through the insulation at the appropriate station.

6. " ΔT ($^\circ\text{K}$)." Inside wall temperature-local saturation temperature at appropriate station.

7. " h_{exp} ($\text{W}/\text{cm}^2\text{-}^\circ\text{K}$)." Heat transfer coefficient $\frac{q}{\Delta T}$.

8. "x" Calculated quality at corresponding station.

9. " $\bar{\rho}$ (g/cc)" Mean density at corresponding station.

$$\frac{1}{\bar{\rho}} = \frac{(1-x)}{\rho_s} + \frac{x}{\rho_{vb}}$$

10. "Nu." See nomenclature.

11. " $h_{\text{exp}}/h_{\text{calc}}$." See nomenclature.

12. "Bo" See nomenclature.

13. "Re" See nomenclature.

Where no numbers occur for a particular station the data for that station were not recorded.

In plotting the graphs from the table some points were not plotted as indicated by the following symbols:

A not plotted in figs. 6 and 9

B not plotted in fig. 4

C not plotted in fig. 9.

Points were not plotted in figs. 6 and 9 when either a quality of 1.0 was reached or the point did not lie on the approximately 45° straight line portion of the q vs ΔT plot. Points were not plotted in fig. 4 if quality of 1.0 was reached or if an abnormally low Reynolds no. pertained.

The numerical values are listed in table 1 in exponent format. This can best be explained by the following example:

$$7.570 - 002 = 7.570 \times 10^{-2} = 0.07570$$

$$3.475 + 001 = 3.475 \times 10^{34.75}$$

For convenience in printing out the results, four significant figures have been given for every measured quantity. However, this often implies an accuracy greater than actually obtained. Reference to the text should be made to determine how far to round off a number.

Table 1. Experimental Results (continued)
.144 cm Orifice (Hydrogen) (continued)

Table with 13 columns: Run, Dischg. Press. (mm Hg), G (g/cm²-sec), Sta, q (W/cm²), ΔT (°K), h_exp (W/cm²-°K), x, β (g/cc), Nu, h_exp/h_calc, Bo, Re. Rows include data for runs 1A, 1, and 1A at various pressure and mass flux conditions.

.105 cm Orifice (Hydrogen)

Table with 13 columns: Run, Dischg. Press. (mm Hg), G (g/cm²-sec), Sta, q (W/cm²), ΔT (°K), h_exp (W/cm²-°K), x, β (g/cc), Nu, h_exp/h_calc, Bo, Re. Rows include data for runs 2, 2, 2, 2, 2, 2, 2, 2, 2, 2, 2, 2, 2, 2, 2, 2, 2, 2, 2, 2 at various pressure and mass flux conditions.

Table 1. Experimental Results (continued)
.059 cm Orifice (Hydrogen) (continued)

Run	Dischg. Press. (mm Hg)	G ($\text{g}/\text{cm}^2\text{-sec}$)	Sta.	q (W/cm^2)	ΔT ($^{\circ}\text{K}$)	h_{exp} ($\text{W}/\text{cm}^2\text{-}^{\circ}\text{K}$)	x	$\bar{\rho}$ (g/cc)	Nu	$h_{\text{exp}}/h_{\text{calc}}$	Bo	Re
4	3.900+000	4.194-002	1	8.025-002	1.184+001	6.778-003	2.395-001	4.951-005	2.054+002	1.159+001	1.640-002	1.957+004
			2	7.738-002	2.211+001	3.500-003	3.051-001	3.976-005	1.057+002	5.172+000	1.241-002	1.952+004
			3	7.280-002	3.857+001	1.888-003	3.678-001	3.299-005	5.703+001	2.505+000	9.684-003	1.952+004
			4	6.922-002	5.147+001	1.345-003	4.273-001	2.776-005	4.075+001	1.648+000	7.929-003	1.957+004
4	4.000+000	4.372-002	1	4.285-002	8.212+000	5.218-003	2.373-001	4.881-005	1.585+002	8.470+000	8.479-003	2.047+004
			2	4.155-002	1.290+001	3.221-003	2.713-001	4.168-005	9.815+001	4.862+000	7.196-003	2.053+004
			3	3.870-002	2.309+001	1.676-003	3.030-001	3.913-005	5.077+001	2.415+000	5.995-003	2.041+004
			4	3.597-002	3.289+001	1.094-003	3.327-001	3.646-005	3.305+001	1.495+000	5.073-003	2.035+004
.144 cm Orifice (Nitrogen)												
5 C	1.400+001	1.773+000	1	3.904-001	1.179+001	3.311-002	2.589-001	7.560-004	1.456+003	1.727+001	3.453-003	1.098+005
			2	3.746-001	6.922+001	5.412-003	2.773-001	6.268-004	2.402+002	2.939+000	3.088-003	1.109+005
			3	3.593-001	1.254+002	2.865-003	2.965-001	4.357-004	1.301+002	1.558+000	2.771-003	1.134+005
			4									
5 C	1.400+001	1.773+000	1	3.904-001	1.179+001	3.311-002	2.589-001	7.560-004	1.456+003	1.727+001	3.453-003	1.098+005
			2	3.745-001	6.966+001	5.376-003	2.773-001	6.268-004	2.386+002	2.921+000	3.087-003	1.109+005
			3	3.593-001	1.254+002	2.865-003	2.965-001	4.357-004	1.301+002	1.558+000	2.771-003	1.134+005
			4									
5 C	1.300+001	1.741+000	1	3.338-001	1.139+001	2.931-002	2.610-001	6.937-004	1.296+003	1.543+001	2.975-003	1.085+005
			2	3.220-001	5.553+001	5.799-003	2.826-001	4.169-004	2.653+002	3.123+000	2.646-003	1.121+005
			3	3.100-001	9.876+001	3.139-003	2.962-001	3.849-004	1.439+002	1.703+000	2.428-003	1.124+005
			4									
5 C	1.300+001	1.741+000	1	3.338-001	1.139+001	2.931-002	2.610-001	6.937-004	1.296+003	1.543+001	2.975-003	1.085+005
			2	3.214-001	5.792+001	5.548-003	2.826-001	4.170-004	2.537+002	2.999+000	2.640-003	1.121+005
			3	3.090-001	1.026+002	3.012-003	2.962-001	3.849-004	1.381+002	1.640+000	2.420-003	1.124+005
			4									
5 C	1.000+001	1.694+000	1	2.800-001	1.042+001	2.448-002	2.647-001	4.408-004	1.221+003	1.421+001	2.495-003	1.083+005
			2	2.719-001	4.014+001	6.774-003	2.845-001	4.007-004	3.105+002	3.617+000	2.279-003	1.093+005
			3	2.587-001	8.873+001	2.916-003	2.985-001	2.789-004	1.373+002	1.607+000	2.072-003	1.121+005
			4									
5 C	1.000+001	1.694+000	1	2.804-001	9.060+000	3.095-002	2.647-001	4.408-004	1.406+003	1.632+001	2.499-003	1.083+005
			2	2.714-001	4.121+001	6.591-003	2.845-001	4.007-004	3.022+002	3.526+000	2.276-003	1.093+005
			3	2.583-001	9.034+001	2.859-003	2.985-001	2.790-004	1.346+002	1.578+000	2.069-003	1.121+005
			4									
5 C	1.000+001	1.694+000	1	2.522-001	1.088+001	2.318-002	2.612-001	5.374-004	1.046+003	1.283+001	2.390-003	1.044+005
			2	2.442-001	4.084+001	5.941-003	2.814-001	3.510-004	2.778+002	3.318+000	2.136-003	1.073+005
			3	2.324-001	8.373+001	2.776-003	2.919-001	2.945-004	1.303+002	1.587+000	1.963-003	1.084+005
			4	2.314-001	8.750+001	2.645-003	3.026-001	2.751-004	1.245+002	1.476+000	1.885-003	1.087+005
5 C	1.000+001	1.694+000	1	2.524-001	1.021+001	2.472-002	2.612-001	5.374-004	1.115+003	1.367+001	2.392-003	1.044+005
			2	2.439-001	4.190+001	5.422-003	2.814-001	3.510-004	2.704+002	3.236+000	2.134-003	1.073+005
			3	2.320-001	8.539+001	2.717-003	2.919-001	2.946-004	1.275+002	1.556+000	1.959-003	1.084+005
			4	2.310-001	8.911+001	2.542-003	3.026-001	2.751-004	1.221+002	1.448+000	1.881-003	1.087+005
5 C	9.000+000	1.584+000	1	2.307-001	2.733+000	8.443-002	2.404-001	2.410-004	4.019+003	4.531+001	2.085-003	1.062+005
			2	2.282-001	1.171+001	1.949-002	2.903-001	2.328-004	9.276+002	1.034+001	1.992-003	1.062+005
			3	2.135-001	6.318+001	3.348-003	2.903-001	3.402-004	1.570+002	1.947+000	1.873-003	1.037+005
			4	2.102-001	7.628+001	2.755-003	3.050-001	2.474-004	1.304+002	1.555+000	1.751-003	1.056+005
5 C	9.000+000	1.584+000	1	2.279-001	1.273+001	1.790-002	2.404-001	2.410-004	8.521+002	9.789+000	2.060-003	1.062+005
			2	2.264-001	1.834+001	1.235-002	2.902-001	2.329-004	5.877+002	6.631+000	1.977-003	1.062+005
			3	2.133-001	6.410+001	3.327-003	2.902-001	3.404-004	1.545+002	1.919+000	1.872-003	1.037+005
			4	2.097-001	7.799+001	2.649-003	3.049-001	2.476-004	1.273+002	1.521+000	1.748-003	1.056+005
5 C	8.500+000	1.636+000	1	2.086-001	1.416+001	1.454+000	2.821-001	2.255-004	6.969+004	7.556+002	1.799-003	1.099+005
			2	2.031-001	1.265+001	1.405-002	2.907-001	2.184-004	7.670+002	8.332+000	1.716-003	1.099+005
			3	1.934-001	4.729+001	4.049-003	2.975-001	2.272-004	1.947+002	2.214+000	1.594-003	1.095+005
			4	1.883-001	6.546+001	2.876-003	3.035-001	2.357-004	1.365+002	1.575+000	1.528-003	1.092+005
5 C	8.500+000	1.636+000	1	2.037-001	1.046+001	1.947-002	2.821-001	2.255-004	9.305+002	1.031+001	1.774-003	1.099+005
			2	2.012-001	1.924+001	1.046-002	2.904-001	2.189-004	5.000+002	5.493+000	1.701-003	1.099+005
			3	1.922-001	5.136+001	3.743-003	2.973-001	2.273-004	1.782+002	2.043+000	1.590-003	1.095+005
			4	1.875-001	6.817+001	2.751-003	3.033-001	2.355-004	1.322+002	1.511+000	1.423-003	1.092+005
5 C	8.500+000	1.636+000	1	1.832-001	-1.225+000	-1.496-001	2.747-001	2.890-004	-7.065-003	-7.877+001	1.649-003	1.085+005
			2	1.796-001	1.191+001	1.508-002	2.823-001	2.812-004	7.118+002	7.980+000	1.572-003	1.085+005
			3	1.753-001	2.818+001	6.223-003	2.976-001	2.804-004	2.995+002	3.267+000	1.449-003	1.106+005
			4	1.699-001	4.719+001	3.400-003	3.011-001	2.376-004	1.709+002	1.931+000	1.390-003	1.091+005
5 C	8.500+000	1.636+000	1	1.811-001	6.323+000	2.445-002	2.746-001	2.890-004	1.353+003	1.534+001	1.630-003	1.085+005
			2	1.781-001	1.721+001	1.035-002	2.822-001	2.813-004	4.887+002	5.530+000	1.560-003	1.085+005
			3	1.716-001	4.174+001	4.111-003	2.974-001	2.005-004	1.978+002	2.213+000	1.419-003	1.106+005
			4	1.688-001	5.122+001	3.249-003	3.004-001	2.379-004	1.564+002	1.781+000	1.382-003	1.091+005
5 C	8.000+000	1.574+000	1	1.624-001	3.119-001	5.245-001	2.799-001	2.414-004	2.478+004	2.798+002	1.482-003	1.053+005
			2	1.590-001	1.230+001	1.293-002	2.870-001	2.355-004	6.156+002	6.983+000	1.416-003	1.053+005
			3	1.596-001	8.845+000	1.804-002	2.844-001	3.473-004	8.380+002	9.694+000	1.441-003	1.028+005
			4	1.529-001	3.441+001	4.443-003	3.007-001	2.247-004	2.115+002	2.406+000	1.299-003	1.053+005
5 C	8.000+000	1.574+000	1	1.603-001	7.777+000	2.061-002	2.799-001	2.414-004	9.811+002	1.126+001	1.463-003	1.053+005
			2	1.576-001	1.760+001	8.950-003	2.860-001	2.356-004	4.260+002	4.878+000	1.403-003	1.053+005
			3	1.567-001	1.940+001	8.075-003	2.842-001	3.475-004	3.750+002	4.419+000	1.416-003	1.028+005
			4	1.517-001	3.882+001	3.907-003	3.004-001	2.249-004	1.860+002	2.134+000	1.290-003	1.053+005

Table 1. Experimental Results (continued)
 .144 cm Orifice (Nitrogen) (continued)

Run	Dischg. Press. (mm Hg)	G (g/cm ² -sec)	Sta.	q (W/cm ²)	ΔT (*K)	h _{exp} (W/cm ² -*K)	x	ρ̄ (g/cc)	Nu	h _{exp} /h _{calc}	Bo	Re	
6	8.000+000	5.291+000	1										
			2										
			3	3.207-001	6.871+001	4.668-003	2.344-001	6.467-004	2.094+002	1.212+000	1.051-003	3.342+005	
			4	3.183-001	8.046+001	3.956-003	2.589-001	2.610-004	1.883+002	9.775-001	9.347-004	3.540+005	
6	8.000+000	5.291+000	1										
			2	3.303-001	3.412+001	9.681-003	2.300-001	6.818-004	4.333+002	2.423+000	1.102-003	3.334+005	
			3	3.207-001	6.871+001	4.668-003	2.344-001	6.467-004	2.094+002	1.212+000	1.051-003	3.342+005	
			4	3.183-001	8.046+001	3.956-003	2.589-001	2.610-004	1.883+002	9.775-001	9.347-004	3.540+005	
6 C	8.500+000	4.192+000	1	2.341-001	7.061+000	3.315-002	2.585-001	5.720-004	1.490+003	8.677+000	8.783-004	2.653+005	
			2	2.359-001	5.574-001	4.232-001	2.624-001	5.636-004	1.902+004	1.081+002	8.719-004	2.653+005	
			3										
			4	2.326-001	1.536+001	1.514-002	2.880-001	2.484-004	7.186+002	3.740+000	7.760-004	2.797+005	
6 C	8.500+000	4.192+000	1	2.326-001	1.248+001	1.864-002	2.585-001	5.720-004	8.379+002	4.926+000	8.726-004	2.653+005	
			2	2.333-001	9.799+000	2.381-002	2.623-001	5.636-004	1.070+003	6.189+000	8.626-004	2.653+005	
			3										
			4	2.296-001	2.597+001	8.843-003	2.879-001	2.485-004	4.198+002	2.228+000	7.666-004	2.797+005	
6 C	9.000+000	4.626+000	1	2.564-001	9.867+000	2.599-002	2.483-001	4.591-004	1.191+003	6.558+000	9.017-004	2.985+005	
			2	2.576-001	5.667+000	4.544-002	2.521-001	4.522-004	2.084+003	1.125+001	8.921-004	2.985+005	
			3	2.572-001	8.296+000	3.100-002	2.590-001	3.214-004	1.460+003	7.599+000	8.491-004	3.062+005	
			4	2.572-001	8.814+000	2.918-002	2.670-001	2.927-004	1.381+003	6.996+000	8.404-004	3.078+005	
6 C	9.000+000	4.626+000	1	2.589-001	1.584+001	1.609-002	2.483-001	4.591-004	7.374+002	4.101+000	9.959-004	2.985+005	
			2	2.557-001	1.256+001	2.036-002	2.521-001	4.422-004	9.336+002	5.101+000	8.855-004	2.985+005	
			3	2.557-001	1.376+001	1.458-002	2.590-001	3.215-004	8.750+002	4.600+000	8.641-004	3.062+005	
			4	2.555-001	1.488+001	1.717-002	2.669-001	2.828-004	8.128+002	4.162+000	8.351-004	3.078+005	
6	8.000+000	4.153+000	1	4.018-001	9.050+000	4.440-002	2.665-001	8.698-004	1.923+003	1.136+001	1.483-003	2.531+005	
			2	3.934-001	4.037+001	9.745-003	2.830-001	6.121-004	4.326+002	2.524+000	1.353-003	2.596+005	
			3	3.829-001	7.872+001	4.864-003	2.910-001	5.338-004	2.178+002	1.302+000	1.287-003	2.619+005	
			4	3.808-001	8.946+001	4.257-003	3.172-001	2.131-004	2.026+002	1.094+000	1.163-003	2.779+005	
6	8.000+000	4.153+000	1	4.010-001	1.170+001	3.428-002	2.665-001	8.698-004	1.485+003	8.810+000	1.480-003	2.531+005	
			2	3.928-001	4.246+001	9.251-003	2.834-001	6.121-004	4.107+002	2.405+000	1.351-003	2.596+005	
			3	3.829-001	7.872+001	4.864-003	2.910-001	5.339-004	2.178+002	1.302+000	1.287-003	2.619+005	
			4	3.808-001	8.946+001	4.257-003	3.172-001	2.131-004	2.026+002	1.094+000	1.163-003	2.779+005	
6 C	9.000+000	4.243+000	1	2.847-001	4.460+000	6.385-002	2.465-001	1.114+003	2.724+003	1.689+001	1.104-003	2.547+005	
			2	2.866-001	4.197+001	6.428-002	2.634-001	5.497-004	3.058+004	1.720+002	1.041-003	2.676+005	
			3	2.747-001	4.285+001	6.412-003	2.680-001	5.796-004	2.872+002	1.721+000	9.815-004	2.676+005	
			4	2.733-001	5.078+001	5.382-003	2.884-001	2.618-004	2.548+002	1.401+000	9.010-004	2.823+005	
6 C	9.000+000	4.243+000	1	2.832-001	9.873+000	2.849-002	2.465-001	1.114+003	1.224+003	7.662+000	1.102-003	2.547+005	
			2	2.842-001	1.233+001	2.297-002	2.634-001	5.497-004	1.029+003	5.916+000	1.030-003	2.676+005	
			3	2.747-001	4.285+001	6.412-003	2.679-001	5.797-004	2.872+002	1.721+000	9.818-004	2.676+005	
			4	2.733-001	5.078+001	5.382-003	2.884-001	2.616-004	2.548+002	1.401+000	9.012-004	2.823+005	
6	1.300+001	5.853+000	1	4.637-001	1.293+001	3.546-002	2.126-001	1.324+003	1.526+003	8.368+000	1.515+003	3.505+005	
			2	4.540-001	5.032+001	9.021-003	2.304-001	6.401-004	4.033+002	2.138+000	1.366-003	3.685+005	
			3	4.424-001	9.156+001	4.432-003	2.354-001	7.383-004	2.145+002	1.175+000	1.302-003	3.659+005	
			4	4.419-001	4.531+001	4.637-003	2.515-001	4.231-004	2.138+002	1.086+000	1.212-003	3.798+005	

.105 cm Orifice (Nitrogen)

7	7.000+000	1.164+000	1	3.308-001	1.008+001	3.281-002	2.694-001	3.377-004	1.534+003	2.351+001	4.265-003	7.657+004	
			2	3.095-001	4.775+001	3.427-003	2.977-001	2.270-004	1.679+002	2.634+000	3.591-003	7.791+004	
			3	2.943-001	1.424+002	2.467-003	3.170-001	2.006-004	9.877+001	1.533+000	3.205-003	7.822+004	
			4	2.901-001	1.578+002	1.839-003	3.346-001	1.783-004	8.850+001	1.319+000	2.996-003	7.877+004	
7	7.000+000	1.164+000	1	3.301-001	1.232+001	2.480-002	2.694-001	3.377-004	1.253+003	1.928+001	4.257-003	7.657+004	
			2	3.091-001	4.918+001	3.466-003	2.977-001	2.270-004	1.650+002	2.592+000	3.587-003	7.791+004	
			3	2.942-001	1.430+002	2.467-003	3.170-001	2.007-004	9.828+001	1.527+000	3.203-003	7.822+004	
			4	2.899-001	1.584+002	1.830-003	3.345-001	1.783-004	8.807+001	1.313+000	2.995-003	7.877+004	
7	8.000+000	1.230+000	1	3.449-001	1.143+001	3.455-002	2.699-001	3.373-004	1.616+003	2.373+001	4.814-003	8.090+004	
			2	3.701-001	1.009+002	3.669-003	2.925-001	2.846-004	1.728+002	2.682+000	4.164-003	8.142+004	
			3	3.541-001	1.586+002	2.233-003	3.129-001	2.661-004	1.051+002	1.607+000	3.725-003	8.142+004	
			4	3.499-001	1.743+002	2.007-003	3.404-001	1.986-004	9.554+001	1.365+000	3.362-003	8.231+004	
7	8.000+000	1.230+000	1	3.944-001	1.324+001	2.978-002	2.699-001	3.373-004	1.393+003	2.052+001	4.808-003	8.090+004	
			2	3.699-001	1.016+002	3.442-003	2.925-001	2.846-004	1.715+002	2.664+000	4.162-003	8.142+004	
			3	3.538-001	1.595+002	2.218-003	3.124-001	2.661-004	1.045+002	1.597+000	3.722-003	8.142+004	
			4	3.496-001	1.754+002	1.993-003	3.403-001	1.986-004	9.488+001	1.357+000	3.359-003	8.231+004	
7	6.500+000	1.104+000	1	4.641-001	1.383+001	3.357-002	2.709-001	3.216-004	1.576+003	2.520+001	4.285-003	7.284+004	
			2	4.320-001	1.302+002	3.319-003	3.079-001	2.195-004	1.580+002	2.606+000	5.113-003	7.386+004	
			3	4.126-001	2.004+002	2.959-003	3.360-001	1.775-004	9.912+001	1.569+000	4.476-003	7.468+004	
			4	4.075-001	2.190+002	1.860-003	3.619-001	1.538-004	9.018+001	1.347+000	4.109-003	7.522+004	
7	6.500+000	1.104+000	1	4.636-001	1.581+001	2.933-002	2.709-001	3.217-004	1.377+003	2.209+001	6.278-003	7.284+004	
			2	4.318-001	1.311+002	3.293-003	3.079-001	2.195-004	1.568+002	2.588+000	5.111-003	7.386+004	
			3	4.125-001	2.008+002	2.054-003	3.360-001	1.776-004	9.887+001	1.569+000	4.475-003	7.468+004	
			4	4.072-001	2.199+002	1.852-003	3.614-001	1.538-004	8.975+001	1.342+000	4.107-003	7.522+004	
7	6.500+000	1.076+000	1	5.393-001	1.581+001	3.411-002	2.726-001	3.454-004	1.606+003	2.611+001	7.441-003	7.124+004	
			2	4.999-001	1.582+002	3.161-003	3.139-001	2.153-004	1.504+002	2.532+000	5.953-003	7.202+004	
			3	4.780-001	2.373+002	2.015-003	3.465-001	1.836-004	9.627+001	1.544+000	5.151-003	7.231+004	
			4	4.686-001	2.717+002	1.725-003	3.775-001	1.474-004	8.359+001	1.257+000	4.645-003	7.334+004	

Table 1. Experimental Results (continued)
 .105 cm Orifice (Nitrogen) (continued)

Run	Dischg. Press. (mm Hg)	G ($g/cm^2\text{-sec}$)	Sta.	q (W/cm^2)	ΔT ($^{\circ}K$)	h_{exp} ($W/cm^2\text{-}^{\circ}K$)	x	$\bar{\rho}$ (g/cc)	Nu	h_{exp}/h_{calc}	Bo	Re
7	6.500+000	1.074+000	1	5.386-001	1.832+001	2.940-002	2.726-001	3.054+004	1.384+003	2.259+001	7.432-003	7.124+004
			2	4.997-001	1.589+002	3.145+003	3.138-001	2.153+004	1.497+002	2.521+000	5.951-003	7.202+004
			3	4.778-001	2.379+002	2.009+003	3.465-001	1.836+004	9.599+001	1.540+000	5.150+003	7.231+004
			4	4.684-001	2.722+002	1.721+003	3.774-001	1.475+004	8.340+001	1.255+000	4.644+003	7.334+004
7	6.500+000	1.042+000	1	6.141-001	1.737+001	3.435+002	2.724-001	3.199+004	1.659+003	2.783+001	8.761-003	6.878+004
			2	5.689-001	1.807+002	3.148+003	3.185-001	2.246+004	1.495+002	2.585+000	6.905+003	6.955+004
			3	5.420-001	2.779+002	1.951+003	3.585-001	1.774+004	9.322+001	1.516+000	5.830+003	7.002+004
			4	5.287-001	3.263+002	1.620+003	3.945-001	1.411+004	7.852+001	1.188+000	5.178+003	7.102+004
7	6.500+000	1.042+000	1	6.133-001	2.023+001	3.031+002	2.724-001	3.199+004	1.423+003	2.398+001	8.750-003	6.878+004
			2	5.686-001	1.820+002	3.124+003	3.184-001	2.247+004	1.483+002	2.567+000	6.902+003	6.955+004
			3	5.416-001	2.792+002	1.940+003	3.584-001	1.775+004	9.271+001	1.508+000	5.827+003	7.002+004
			4	5.283-001	3.275+002	1.613+003	3.945-001	1.411+004	7.819+001	1.183+000	5.176+003	7.102+004
7	7.000+000	1.070+000	1	6.864-001	1.802+001	3.809+002	2.734-001	3.040+004	1.793+003	2.930+001	4.485+003	7.081+004
			2	6.357-001	2.006+002	3.169+003	3.224-001	2.219+004	1.504+002	2.547+000	7.426+003	7.139+004
			3	6.052-001	3.109+002	1.946+003	3.656-001	1.740+004	9.301+001	1.471+000	6.219+003	7.187+004
			4	5.903-001	3.648+002	1.618+003	4.043-001	1.475+004	7.788+001	1.148+000	5.490+003	7.238+004
7	7.000+000	1.070+000	1	6.854-001	2.168+001	3.161+002	2.734-001	3.041+004	1.489+003	2.447+001	9.472+003	7.081+004
			2	6.355-001	2.016+002	3.152+003	3.223+001	2.219+004	1.496+002	2.535+000	7.424+003	7.139+004
			3	6.045-001	3.134+002	1.929+003	3.655-001	1.740+004	9.217+001	1.460+000	6.213+003	7.187+004
			4	5.899-001	3.661+002	1.611+003	4.042+001	1.476+004	7.755+001	1.144+000	5.488+003	7.238+004
7	6.500+000	1.062+000	1	2.727-001	8.171+000	3.138+002	2.746+001	2.749+004	1.580+003	2.536+001	3.774+003	7.068+004
			2	2.538-001	7.704+001	3.294+003	2.975-001	2.005+004	1.586+002	2.631+000	3.232+003	7.186+004
			3	2.372-001	1.371+002	1.729+003	3.137+001	1.774+004	8.383+001	1.394+000	2.467+003	7.237+004
			4									
7	6.500+000	1.062+000	1	2.719-001	1.130+001	2.405+002	2.746+001	2.749+004	1.139+003	1.838+001	3.762+003	7.068+004
			2	2.531-001	7.898+001	3.207+003	2.974+001	2.005+004	1.543+002	2.567+000	3.226+003	7.186+004
			3	2.369-001	1.381+002	1.715+003	3.136+001	1.775+004	8.313+001	1.384+000	2.864+003	7.237+004
			4									

.069 cm Orifice (Nitrogen)

8	6.500+000	7.184+001	1	4.955-001	1.123+002	4.411+003	2.775-001	2.804+004	2.085+002	5.227+000	1.004+002	4.773+004	
			2										
			3	4.355-001	3.289+002	1.744+003	3.783+001	1.702+004	6.310+001	1.346+000	6.438+003	4.819+004	
			4	4.194-001	3.871+002	1.084+003	4.201+001	1.325+004	5.252+001	1.034+000	5.598+003	4.895+004	
8	6.000+000	6.914+001	1	5.688-001	1.009+002	5.640+003	2.806-001	2.549+004	2.677+002	6.771+000	1.180+002	4.616+004	
			2	5.286-001	2.454+002	2.154+003	3.371+001	2.005+004	1.025+002	2.409+000	9.119+003	4.629+004	
			3	5.048-001	3.313+002	1.574+003	3.887+001	1.718+004	7.258+001	1.562+000	7.549+003	4.631+004	
			4	4.812-001	4.171+002	1.154+003	4.401+001	1.173+004	5.632+001	1.105+000	6.373+003	4.748+004	
8	6.000+000	7.613+001	1	5.358-001	9.146+001	5.858+003	2.797+001	2.558+004	2.781+002	6.479+000	1.014+002	5.080+004	
			2	4.970-001	2.310+002	2.152+003	3.275+001	2.112+004	1.023+002	2.268+000	8.025+003	5.089+004	
			3	4.762-001	3.060+002	1.556+003	3.721+001	1.816+004	7.408+001	1.519+000	6.762+003	5.094+004	
			4	4.548-001	3.766+002	1.213+003	4.169+001	1.238+004	5.922+001	1.111+000	5.804+003	5.225+004	
8	5.500+000	7.406+001	1	5.187-001	8.386+001	6.185+003	2.821+001	2.367+004	2.946+002	6.903+000	9.983+003	4.958+004	
			2	4.865-001	2.211+002	2.173+003	3.295+001	1.931+004	1.039+002	2.326+000	7.915+003	4.975+004	
			3	4.617-001	2.887+002	1.599+003	3.724+001	1.772+004	7.628+001	1.587+000	6.730+003	4.961+004	
			4	4.424-001	3.593+002	1.231+003	4.170+001	1.141+004	6.052+001	1.150+000	5.779+003	5.119+004	
8	6.000+000	7.833+001	1	5.057-001	8.253+001	6.128+003	2.791+001	2.563+004	2.909+002	6.581+000	9.321+003	5.227+004	
			2	4.686-001	2.161+002	2.168+003	3.242+001	2.086+004	1.033+002	2.241+000	7.422+003	5.244+004	
			3	4.507-001	2.806+002	1.608+003	3.641+001	1.856+004	7.646+001	1.548+000	6.358+003	5.241+004	
			4	4.319-001	3.490+002	1.238+003	4.055+001	1.273+004	6.043+001	1.125+000	5.484+003	5.376+004	
8	5.000+000	7.134+001	1	4.272-001	9.538+001	4.479+002	2.823+001	2.113+004	2.156+003	4.606+001	8.535+003	4.826+004	
			2	3.802-001	1.787+002	2.128+003	3.215+001	1.731+004	1.032+002	2.362+000	6.678+003	4.861+004	
			3	3.645-001	2.348+002	1.553+003	3.570+001	1.671+004	7.472+001	1.617+000	5.760+003	4.826+004	
			4	3.489-001	2.923+002	1.193+003	3.944+001	1.103+004	5.903+001	1.181+000	5.000+003	4.964+004	
8	5.000+000	7.439+001	1	3.958-001	8.172+001	4.843+002	2.821+001	2.114+004	2.331+003	4.807+001	7.588+003	5.032+004	
			2	3.521-001	1.657+002	2.125+003	3.172+001	1.679+004	1.034+002	2.296+000	6.015+003	5.091+004	
			3	3.384-001	2.149+002	1.575+003	3.492+001	1.502+004	7.677+001	1.610+000	5.253+003	5.098+004	
			4	3.263-001	2.590+002	1.260+003	3.823+001	1.139+004	6.231+001	1.225+000	4.628+003	5.176+004	
8	4.900+000	7.100+001	1	2.612-001	6.039+001	4.325+002	2.807+001	1.983+004	2.097+003	4.465+001	5.279+003	4.838+004	
			2	2.314-001	1.136+002	2.038+003	3.056+001	1.557+004	1.002+002	2.286+000	4.304+003	4.907+004	
			3	2.239-001	1.404+002	1.585+003	3.271+001	1.503+004	7.819+001	1.726+000	3.890+003	4.894+004	
			4	2.132-001	1.794+002	1.188+003	3.507+001	1.218+004	5.885+001	1.244+000	3.453+003	4.947+004	
8	5.000+000	7.614+001	1	1.529-001	4.537+001	3.371+002	2.794+001	2.049+004	1.629+003	3.290+001	2.894+003	5.173+004	
			2	1.355-001	6.795+001	1.994+003	2.935+001	1.621+004	9.800+001	2.094+000	2.446+003	5.263+004	
			3	1.327-001	7.774+001	1.707+003	3.051+001	1.639+004	8.357+001	1.754+000	2.304+003	5.241+004	
			4	1.271-001	1.162+002	1.051+003	3.187+001	1.365+004	5.198+001	1.082+000	2.029+003	5.298+004	
8	4.800+000	7.280+001	1	1.084-001	3.956+001	2.740+002	2.794+001	1.847+004	1.338+003	2.776+001	2.148+003	4.997+004	
			2	9.641+002	4.723+001	2.041+003	2.898+001	1.641+004	1.004+002	2.177+000	1.844+003	5.032+004	
			3	9.708+002	4.498+001	2.158+003	2.996+001	1.534+004	1.064+002	2.234+000	1.795+003	5.046+004	
			4	8.530+002	8.762+001	9.735+004	3.098+001	1.352+004	4.827+001	1.038+000	1.525+003	5.079+004	

Table 1. Experimental Results (continued)

.089 cm Orifice (Nitrogen) (continued)

Run	Dischg. Press. (mm Hg)	G (g/cm^2 -sec)	Sta.	q (W/cm^2)	ΔT ($^{\circ}K$)	h_{exp} (W/cm^2 - $^{\circ}K$)	x	$\bar{\rho}$ (g/cc)	Nu	h_{exp}/h_{calc}	Bo	Re
8	4.500+000	7.456-001	1	9.179-002	2.692+000	3.409-002	2.795-001	1.759-004	1.672+003	3.383+001	1.777-003	5.139+004
			2	8.398-002	3.120+001	2.691-003	2.897-001	1.502-004	1.331+002	2.742+000	1.568-003	5.188+004
			3	8.721-002	1.900+001	4.590+003	2.953-001	1.748-004	2.241+002	4.486+000	1.597+003	5.117+004
			4	7.572-002	6.123+001	1.237-003	3.067-001	1.285-004	6.155+001	1.269+000	1.334-003	5.223+004
8	6.000+000	7.103-001	1	5.297-001	2.342+002	2.262-003	3.369-001	2.006-004	1.077+002	2.467+000	8.904-003	4.752+004
			2	5.021-001	3.334+002	1.506-003	3.872-001	1.725-004	7.173+001	1.517+000	7.344-003	4.755+004
			3	4.807-001	4.113+002	1.169-003	4.371-001	1.181-004	5.706+001	1.100+000	6.244-003	4.875+004
			4									

.059 cm Orifice (Nitrogen)

9	5.000+000	3.137-001	1	2.735-001	6.391+000	4.280-002	2.896-001	1.503-004	2.117+003	8.329+001	1.214-002	2.183+004
			2	2.294-001	1.651+002	1.389-003	3.447-001	1.267-004	6.872+001	2.812+000	8.553-003	2.183+004
			3	2.157-001	2.143+002	1.006-003	3.935-001	1.106-004	4.978+001	1.874+000	7.045-003	2.183+004
			4	2.044-001	2.549+002	8.020-004	4.396-001	9.901-005	3.967+001	1.388+000	5.977-003	2.183+004
9	5.000+000	3.137-001	1	2.724-001	1.057+001	2.576-002	2.895-001	1.503-004	1.274+003	5.053+001	1.209-002	2.183+004
			2	2.294-001	1.651+002	1.389-003	3.446-001	1.263-004	6.872+001	2.813+000	8.557-003	2.183+004
			3	2.157-001	2.143+002	1.006-003	3.933-001	1.106-004	4.978+001	1.874+000	7.048-003	2.183+004
			4	2.044-001	2.549+002	8.020-004	4.394-001	9.905-005	3.967+001	1.389+000	5.979-003	2.183+004
9	5.000+000	2.956-001	1	1.811-001	5.315+000	3.408-002	2.871-001	1.516-004	1.685+003	6.990+001	8.607-003	2.057+004
			2	1.474-001	1.447+002	9.839-004	3.247-001	1.340-004	4.867+001	2.171+000	5.981-003	2.057+004
			3	1.315-001	1.835+002	7.168-004	3.566-001	1.221-004	3.545+001	1.495+000	5.033-003	2.057+004
			4	1.223-001	2.168+002	5.640-004	3.861-001	1.127-004	2.790+001	1.119+000	4.321-003	2.057+004
9	5.000+000	2.956-001	1	1.801-001	8.972+000	2.007-002	2.870-001	1.516-004	9.928-002	4.147+001	8.560-003	2.057+004
			2	1.474-001	1.447+002	9.839-004	3.245-001	1.341-004	4.867+001	2.171+000	5.984-003	2.057+004
			3	1.315-001	1.835+002	7.168-004	3.564-001	1.221-004	3.545+001	1.495+000	5.035-003	2.057+004
			4	1.223-001	2.168+002	5.640-004	3.860-001	1.128-004	2.790+001	1.120+000	4.323-003	2.057+004
9	5.000+000	3.450-001	1	1.829-001	4.761+000	3.842-002	2.867-001	1.518-004	1.900+003	6.964+001	7.458-003	2.400+004
			2	1.503-001	1.221+002	1.231-003	3.199-001	1.360-004	6.087+001	2.391+000	5.491-003	2.400+004
			3	1.417-001	1.531+002	9.256-004	3.490-001	1.247-004	4.578+001	1.710+000	4.745-003	2.400+004
			4	1.317-001	1.889+002	6.973-004	3.763-001	1.157-004	3.449+001	1.234+000	4.092-003	2.400+004
9	5.000+000	3.450-001	1	1.821-001	7.717+000	2.360-002	2.867-001	1.518-004	1.167+003	4.302+001	7.425-003	2.400+004
			2	1.503-001	1.221+002	1.231-003	3.198-001	1.361-004	6.087+001	2.391+000	5.491-003	2.400+004
			3	1.417-001	1.531+002	9.256-004	3.489-001	1.247-004	4.578+001	1.710+000	4.746-003	2.400+004
			4	1.317-001	1.889+002	6.973-004	3.762-001	1.157-004	3.449+001	1.234+000	4.093-003	2.400+004
9	5.000+000	2.980-001	1	1.735-001	4.211+000	4.120-002	2.875-001	1.514-004	2.038+003	8.367+001	8.165-003	2.074+004
			2	1.421-001	1.137+002	1.258-003	3.240-001	1.343-004	6.222+001	2.701+000	5.973-003	2.074+004
			3	1.357-001	1.401+002	9.691-004	3.562-001	1.222-004	4.793+001	1.966+000	5.155-003	2.074+004
			4	1.258-001	1.756+002	7.164-004	3.864-001	1.126-004	3.543+001	1.388+000	4.406-003	2.074+004
9	5.000+000	2.980-001	1	1.724-001	8.133+000	2.120-002	2.875-001	1.514-004	1.048+003	4.338+001	8.115-003	2.074+004
			2	1.431-001	1.137+002	1.258-003	3.239-001	1.344-004	6.222+001	2.703+000	5.976-003	2.074+004
			3	1.357-001	1.401+002	9.691-004	3.561-001	1.222-004	4.793+001	1.967+000	5.158-003	2.074+004
			4	1.258-001	1.756+002	7.164-004	3.862-001	1.127-004	3.543+001	1.387+000	4.408-003	2.074+004
9	5.000+000	3.483-001	1	1.538-001	3.661+000	4.202-002	2.860-001	1.522-004	2.079+003	7.226+001	5.889+003	2.563+004
			2	1.269-001	1.007+002	1.260-003	3.122-001	1.394-004	6.234+001	2.729+000	6.449-003	2.563+004
			3	1.206-001	1.233+002	9.781-004	3.353-001	1.298-004	4.838+001	1.738+000	3.937-003	2.563+004
			4	1.102-001	1.605+002	6.867-004	3.568-001	1.220-004	3.396+001	1.186+000	3.381-003	2.563+004
9	5.000+000	3.483-001	1	1.530-001	4.642+000	2.297-002	2.860-001	1.522-004	1.136+003	3.973+001	5.857-003	2.563+004
			2	1.269-001	1.007+002	1.260-003	3.121-001	1.394-004	6.234+001	2.729+000	6.450-003	2.563+004
			3	1.206-001	1.233+002	9.781-004	3.352-001	1.298-004	4.838+001	1.738+000	3.938-003	2.563+004
			4	1.102-001	1.605+002	6.867-004	3.567-001	1.220-004	3.396+001	1.187+000	3.382-003	2.563+004
9	5.000+000	2.901-001	1	1.357-001	9.644+000	1.407-002	2.870-001	1.516-004	4.959+002	2.954+001	6.571-003	2.019+004
			2	1.128-001	9.182+001	1.229-003	3.165-001	1.375-004	6.077+001	2.697+000	4.955-003	2.019+004
			3	1.083-001	1.080+002	1.003-003	3.427-001	1.270-004	4.963+001	2.095+000	4.394-003	2.019+004
			4	9.822-002	1.443+002	6.806-004	3.672-001	1.185-004	3.364+001	1.381+000	3.718-003	2.019+004
9	5.000+000	2.901-001	1	1.348-001	1.279+001	1.058-002	2.870-001	1.516-004	5.213+002	2.226+001	6.529-003	2.019+004
			2	1.128-001	9.182+001	1.229-003	3.163-001	1.376-004	6.077+001	2.698+000	4.957-003	2.019+004
			3	1.083-001	1.080+002	1.003-003	3.426-001	1.270-004	4.963+001	2.096+000	4.396-003	2.019+004
			4	9.822-002	1.443+002	6.806-004	3.670-001	1.184-004	3.366+001	1.381+000	3.720-003	2.019+004
9	5.000+000	3.786-001	1	1.041-001	2.759+000	3.775-002	2.854-001	1.525-004	1.867+003	6.745+001	3.887-003	2.634+004
			2	8.539-002	7.019+001	1.217-003	3.026-001	1.438-004	6.017+001	2.190+000	3.005-003	2.634+004
			3	8.394-002	7.541+001	1.113-003	3.188-001	1.369-004	5.506+001	1.936+000	2.812-003	2.634+004
			4	7.317-002	1.141+002	6.411-004	3.323-001	1.310-004	3.171+001	1.115+000	2.746-003	2.634+004
9	5.000+000	3.786-001	1	1.033-001	5.796+000	1.782-002	2.854-001	1.525-004	8.816+002	3.016+001	3.856-003	2.634+004
			2	8.539-002	7.019+001	1.217-003	3.025-001	1.439-004	6.017+001	2.190+000	3.006-003	2.634+004
			3	8.394-002	7.541+001	1.113-003	3.179-001	1.369-004	5.506+001	1.937+000	2.812-003	2.634+004
			4	7.317-002	1.141+002	6.411-004	3.322-001	1.310-004	3.171+001	1.115+000	2.746-003	2.634+004
9	5.000+000	3.787-001	1	6.815-002	9.592+000	7.105-003	2.841-001	1.532-004	3.514+002	1.215+001	2.554-003	2.635+004
			2	5.732-002	4.853+001	1.181-003	2.955-001	1.473-004	5.842+001	2.100+000	2.065-003	2.635+004
			3	5.937-002	4.116+001	1.443-003	3.061-001	1.422-004	7.135+001	2.461+000	2.065-003	2.635+004
			4	4.785-002	8.256+001	5.796-004	3.159-001	1.378-004	2.867+001	1.021+000	1.613-003	2.635+004
9	5.000+000	3.787-001	1	6.776-002	1.100+001	6.157-003	2.841-001	1.532-004	3.045+002	1.056+001	2.539-003	2.635+004
			2	5.732-002	4.853+001	1.181-003	2.955-001	1.473-004	5.842+001	2.100+000	2.066-003	2.635+004
			3	5.937-002	4.116+001	1.443-003	3.061-001	1.422-004	7.135+001	2.461+000	2.065-003	2.635+004
			4	4.785-002	8.256+001	5.796-004	3.158-001	1.378-004	2.867+001	1.021+000	1.613-003	2.635+004

Table 1. Experimental Results (continued)
 .059 cm Orifice (Nitrogen) (continued)

Run	Dischg. Press. (mm Hg)	G (g/cm ² -sec)	Sta.	q (W/cm ²)	ΔT (*K)	h_{exp} (W/cm ² -*K)	x	$\bar{\rho}$ (g/cc)	Nu	h_{exp}/h_{calc}	Bo	Re	
10	5.000+000	2.749-001	1	2.907-001	1.279+002	2.273-003	2.898-001	1.502-004	1.124+002	5.753+000	1.471-002	1.913+004	
			2	2.637-001	2.250+002	1.172-003	3.592-001	1.212-004	5.795+001	2.618+000	1.077-002	1.913+004	
			3	2.500-001	2.741+002	9.122-004	4.234-001	1.028-004	4.512+001	1.820+000	8.660-003	1.913+004	
			4	2.349-001	3.285+002	7.150-004	4.841-001	8.990-005	3.537+001	1.302+000	7.117-003	1.913+004	
10	5.000+000	1.902-001	1	3.063-001	1.376+002	2.227-003	2.951-001	1.475-004	1.101+002	7.511+000	2.201-002	1.323+004	
			2	2.814-001	2.272+002	1.238-003	4.014-001	1.084-004	6.125+001	3.403+000	1.487-002	1.323+004	
			3	2.629-001	2.940+002	8.941-004	4.999-001	8.707-005	4.422+001	2.109+000	1.115-002	1.323+004	
			4	2.438-001	3.625+002	6.725-004	5.915-001	7.358-005	3.326+001	1.413+000	8.740-003	1.323+004	
10	5.000+000	2.514-001	1	2.298-001	1.039+002	2.212-003	2.889-001	1.507-004	1.094+002	5.917+000	1.276-002	1.750+004	
			2	2.098-001	1.758+002	1.193-003	3.490-001	1.247-004	5.902+001	2.870+000	9.640-003	1.750+004	
			3	1.994-001	2.129+002	9.365-004	4.049-001	1.075-004	4.632+001	2.033+000	7.898-003	1.750+004	
			4	1.898-001	2.476+002	7.664-004	4.582-001	9.499-005	3.791+001	1.527+000	6.643-003	1.750+004	
10	5.000+000	2.090-001	1	2.075-001	9.275+001	2.237-003	2.893-001	1.504-004	1.106+002	6.844+000	1.379-002	1.460+004	
			2	1.896-001	1.571+002	1.207-003	3.544-001	1.228-004	5.968+001	3.284+000	1.028-002	1.460+004	
			3	1.811-001	1.877+002	9.648-004	4.152-001	1.048-004	4.772+001	2.348+000	4.384-003	1.460+004	
			4	1.716-001	2.219+002	7.734-004	4.730-001	9.201-005	3.825+001	1.719+000	6.973-003	1.460+004	
10	5.000+000	2.280-001	1	1.579-001	7.926+001	1.992-003	2.868-001	1.517-004	9.851+001	5.667+000	9.734-003	1.587+004	
			2	1.419-001	1.366+002	1.039-003	3.320-001	1.311-004	5.139+001	2.757+000	7.559-003	1.587+004	
			3	1.354-001	1.601+002	8.459-004	3.738-001	1.164-004	4.184+001	2.066+000	4.405-003	1.587+004	
			4	1.256-001	1.954+002	6.425-004	4.132-001	1.053-004	3.178+001	1.474+000	5.374-003	1.587+004	
10	4.000+000	1.355-001	1	9.496-002	6.977+001	1.361-003	2.904-001	1.215-004	6.823+001	5.778+000	9.719-003	9.563+003	
			2	8.479-002	1.063+002	7.976-004	3.360-001	1.050-004	3.998+001	3.119+000	7.502-003	9.563+003	
			3	8.271-002	1.138+002	7.266-004	3.785-001	9.322-005	3.643+001	2.599+000	6.496-003	9.563+003	
			4	7.256-002	1.503+002	4.828-004	4.179-001	8.444-005	2.420+001	1.636+000	5.162-003	9.563+003	
10	4.000+000	1.175-001	1	8.009-002	5.905+001	1.356-003	2.902-001	1.216-004	6.800+001	6.370+000	9.460-003	8.294+003	
			2	7.052-002	9.347+001	7.545-004	3.342-001	1.056-004	3.782+001	3.284+000	7.232-003	8.294+003	
			3	7.016-002	9.478+001	7.402-004	3.753-001	9.401-005	3.711+001	2.940+000	6.407-003	8.294+003	
			4	6.016-002	1.307+002	4.602-004	4.134-001	8.534-005	2.307+001	1.741+000	4.988-003	8.294+003	
10	4.000+000	1.455-001	1	6.726-002	3.592+001	1.873-003	2.878-001	1.226-004	9.388+001	6.471+000	5.689-003	1.168+004	
			2	5.784-002	6.978+001	8.289-004	3.137-001	1.125-004	4.155+001	2.820+000	4.487-003	1.168+004	
			3	5.980-002	6.271+001	9.536-004	3.382-001	1.043-004	4.781+001	3.030+000	4.305-003	1.168+004	
			4	4.902-002	1.015+002	4.830-004	3.608-001	9.780-005	2.421+001	1.514+000	3.307-003	1.168+004	
10	4.000+000	1.159-001	1	5.114-002	2.279+001	2.244-003	2.884-001	1.223-004	1.125+002	1.004+001	6.161-003	8.182+003	
			2	4.372-002	4.949+001	8.834-004	3.166-001	1.115-004	4.429+001	3.851+000	4.798-003	8.182+003	
			3	4.848-002	3.237+001	1.497-003	3.439-001	1.026-004	7.507+001	5.927+000	4.898-003	8.182+003	
			4	3.614-002	7.674+001	4.710-004	3.690-001	9.563-005	2.361+001	1.884+000	3.403-003	8.182+003	
10	4.000+000	1.159-001	1	4.786-002	2.005+001	2.387-003	2.883-001	1.224+004	1.197+002	1.063+001	5.769-003	8.181+003	
			2	4.114-002	4.424+001	9.298-004	3.147-001	1.121-004	4.661+001	4.035+000	4.543-003	8.181+003	
			3	4.657-002	2.472+001	1.884-003	3.406-001	1.036-004	9.445+001	7.400+000	4.750-003	8.181+003	
			4	3.372-002	7.092+001	4.754-004	3.644-001	9.681-005	2.383+001	1.910+000	3.215-003	8.181+003	
10	4.000+000	4.125-002	1	4.839-002	1.152+001	4.201-003	2.899-001	1.217-004	2.106+002	2.438+001	4.275-003	5.735+003	
			2	3.997-002	4.181+001	9.558-004	3.272-001	1.078-004	4.792+001	5.319+000	6.054-003	5.735+003	
			3	4.404-002	1.997+001	2.306-003	3.636-001	9.704-005	1.156+002	1.133+001	6.277-003	5.735+003	
			4	3.317-002	6.624+001	5.008-004	3.971-001	8.885-005	2.511+001	2.483+000	4.141-003	5.735+003	
10	4.000+000	5.831-002	1	3.070-002	2.922+000	1.034-002	2.895-001	1.219-004	5.181+002	7.693+001	7.705-003	4.116+003	
			2	2.337-002	2.748+001	8.503-004	3.210-001	1.099-004	4.263+001	6.102+000	5.027-003	4.116+003	
			3										
			4	1.791-002	4.709+001	3.804-004	3.843-001	9.181-005	1.907+001	2.450+000	3.219-003	4.116+003	

Table 2. Orifice Discharge Coefficients

Fluid	Orifice dia (cm)	Orifice Reynolds no. ($\times 10^{-3}$)	$\beta = \frac{\text{dia of orifice}}{\text{dia upstream of orifice}}$	Discharge Coefficient
H ₂	0.144	171 - 191	0.075	0.40 - 0.45
H ₂	0.105	147 - 223	0.055	0.48 - 0.71
H ₂	0.089	120 - 140	0.047	0.39 - 0.53
H ₂	0.059	17 - 47	0.031	0.10 - 0.27
N ₂	0.144	98 - 138	0.075	0.53 - 0.58
N ₂	0.144	37 - 39	0.075	0.37 - 0.39
N ₂	0.105	34 - 40	0.055	0.47 - 0.55
N ₂	0.089	27 - 29	0.047	0.44 - 0.49
N ₂	0.059	17 - 22	0.031	0.43 - 0.56
N ₂	0.059	3 - 16	0.031	0.08 - 0.41

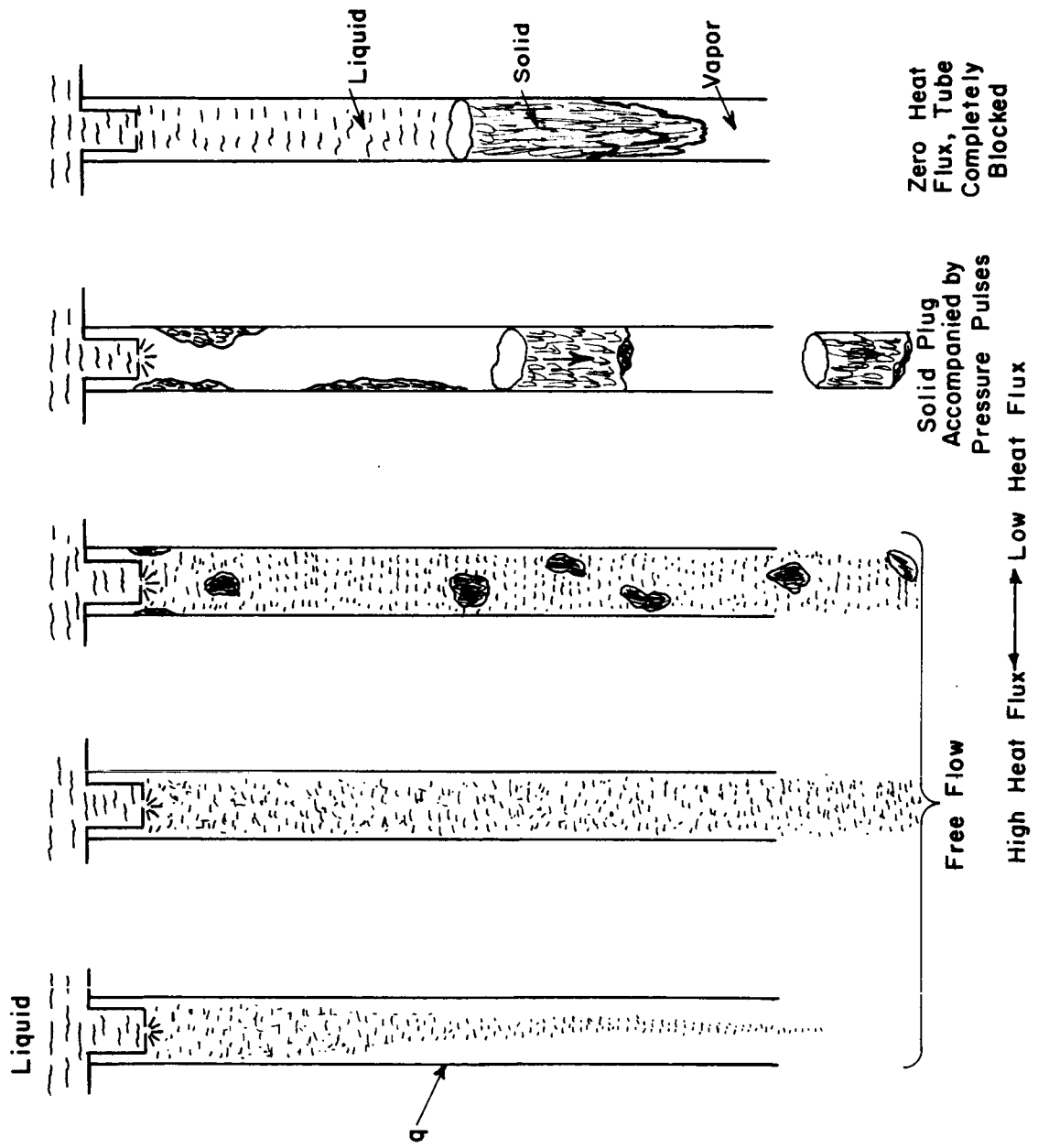


Fig. 1. Illustration of observed behavior of solid-vapor mixture discharging from test section.

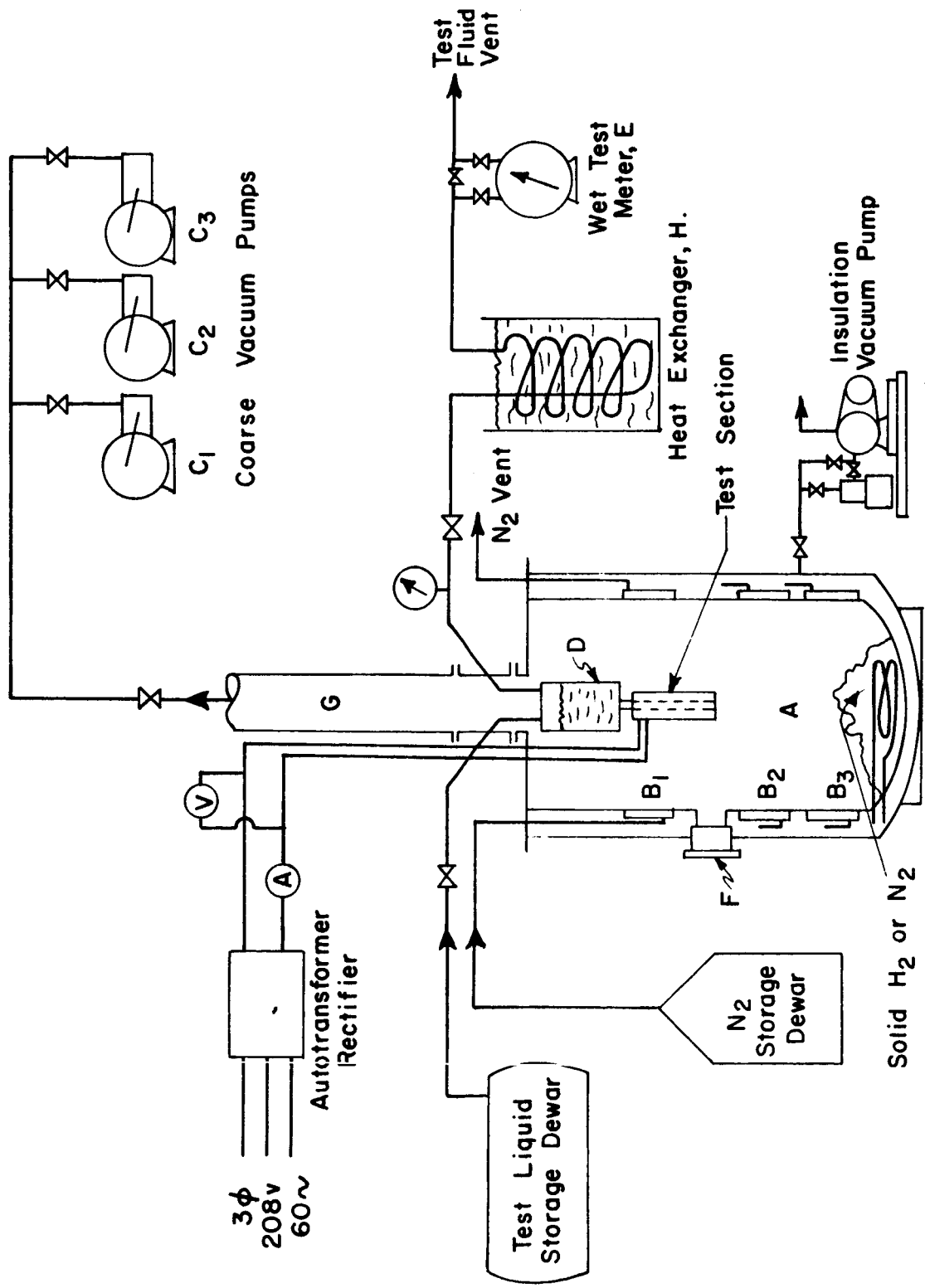


Fig. 2. Schematic arrangement of experimental system.

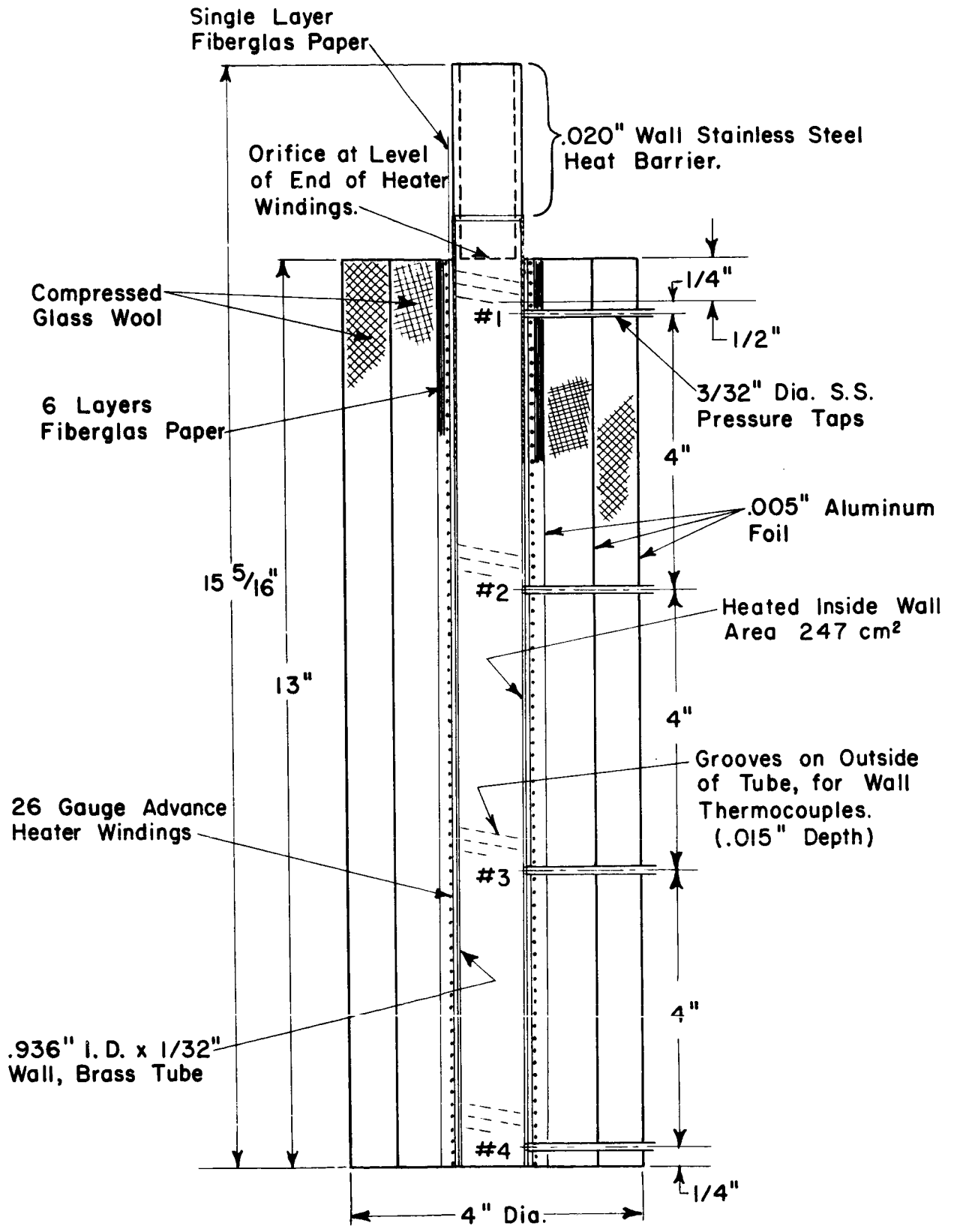


Fig. 3. Heated brass test section.

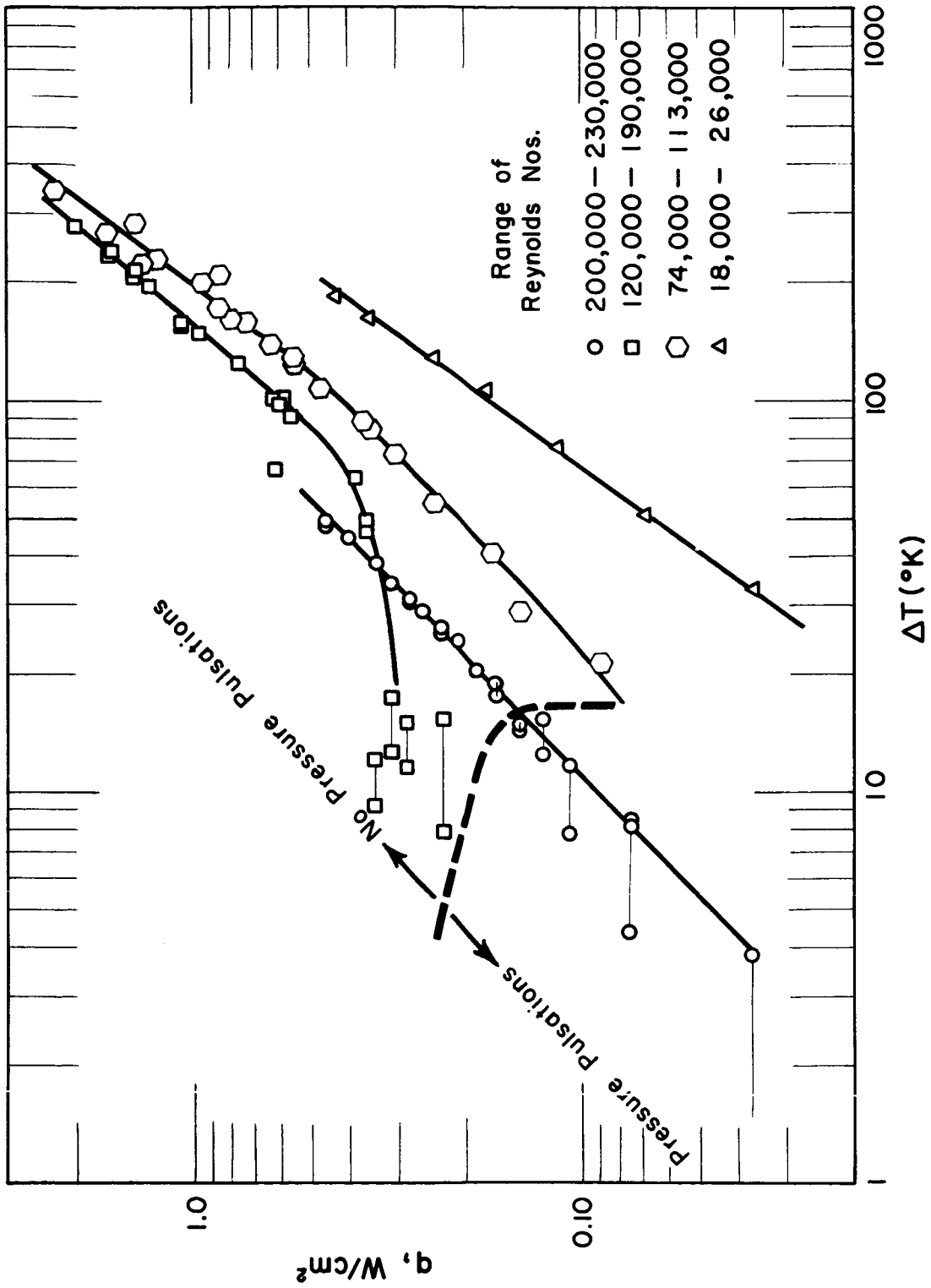


Fig. 4. Heat flux vs temperature difference at station 4. (HYDROGEN)

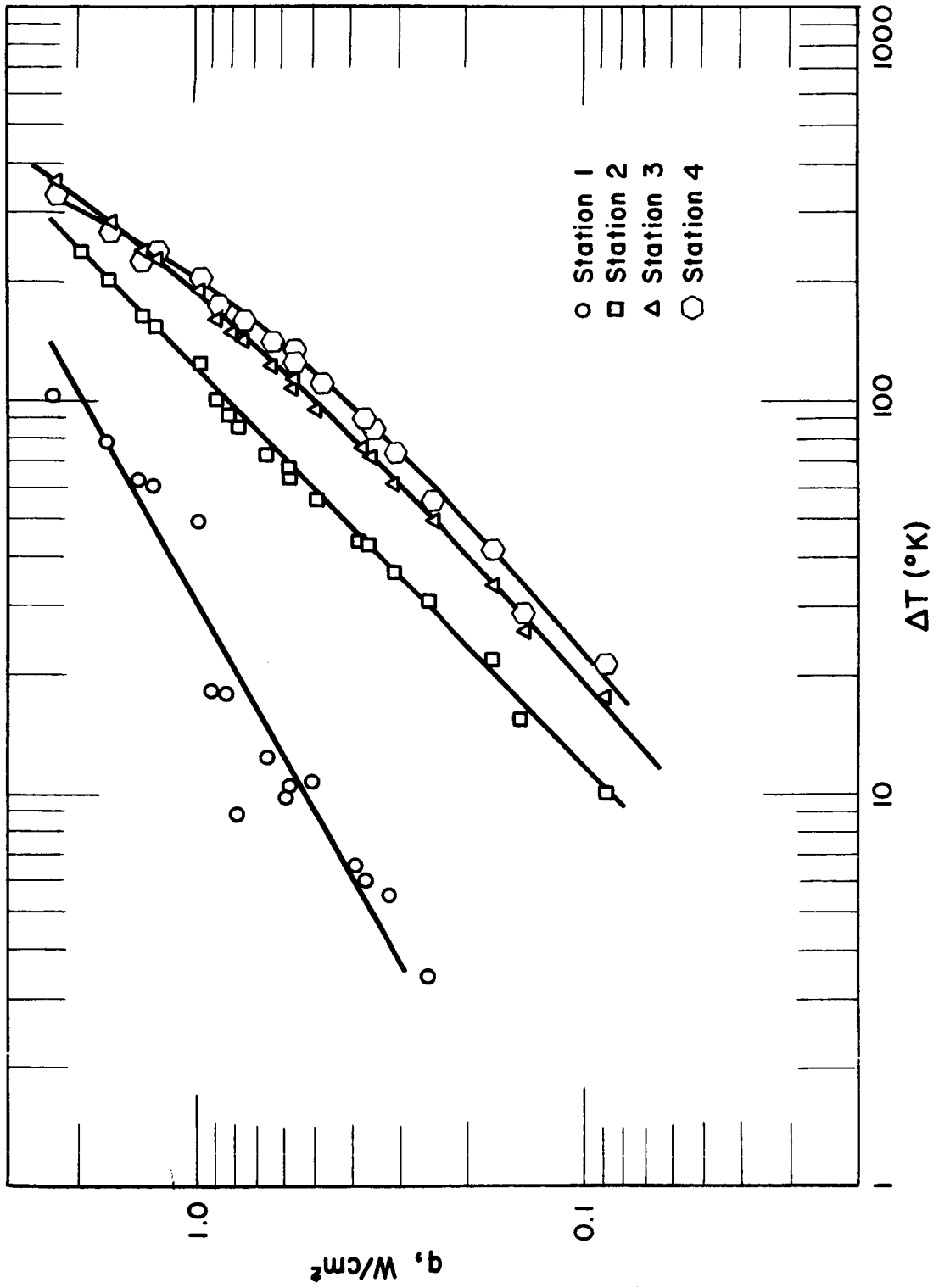


Fig. 5. Heat flux vs temperature difference. Range of Reynolds numbers
 74,000-113,000. (HYDROGEN)

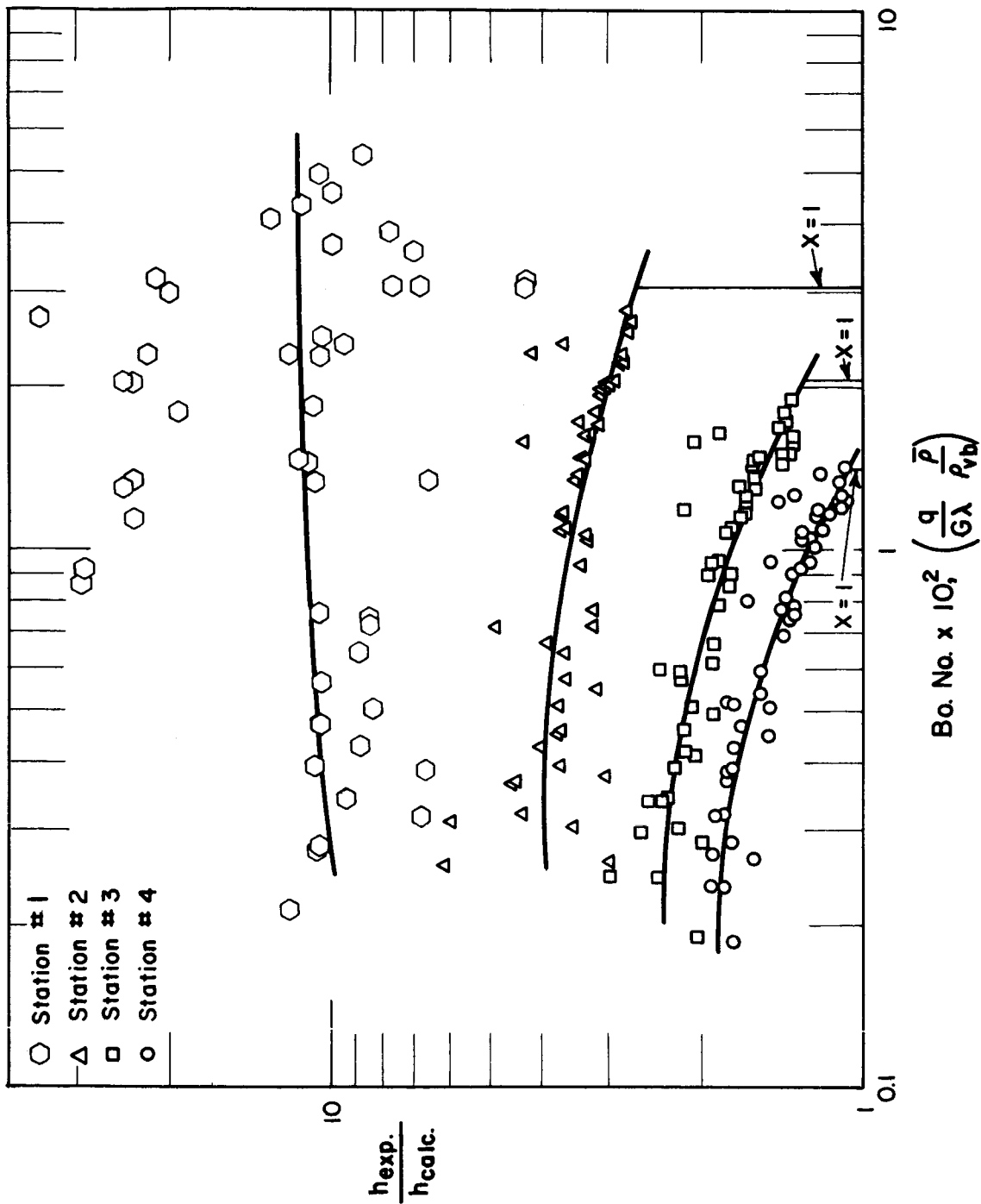


Fig. 6. Heat transfer coefficient ratio vs Boiling number at stations 1, 2, 3, and 4. Reynolds number range 18,000-230,000. (HYDROGEN)

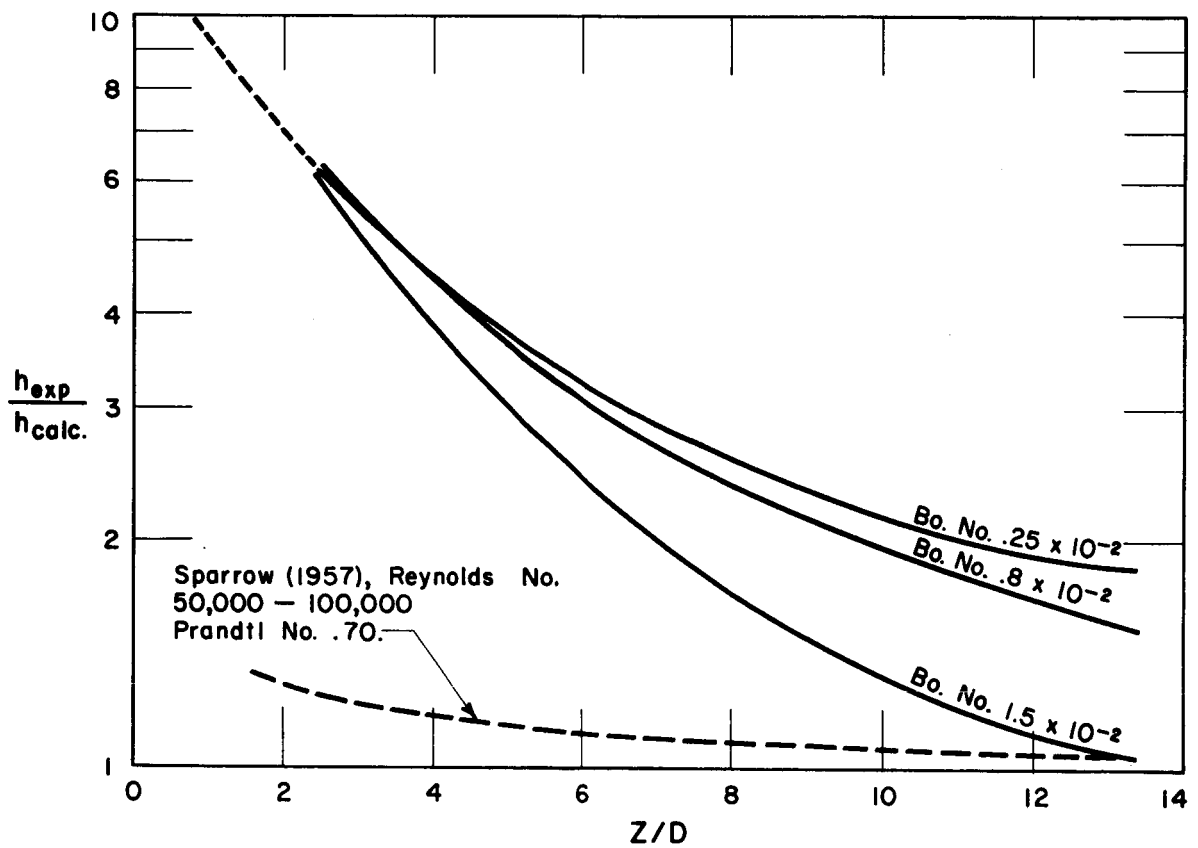


Fig. 7. Heat transfer coefficient ratio vs axial distance. (HYDROGEN)

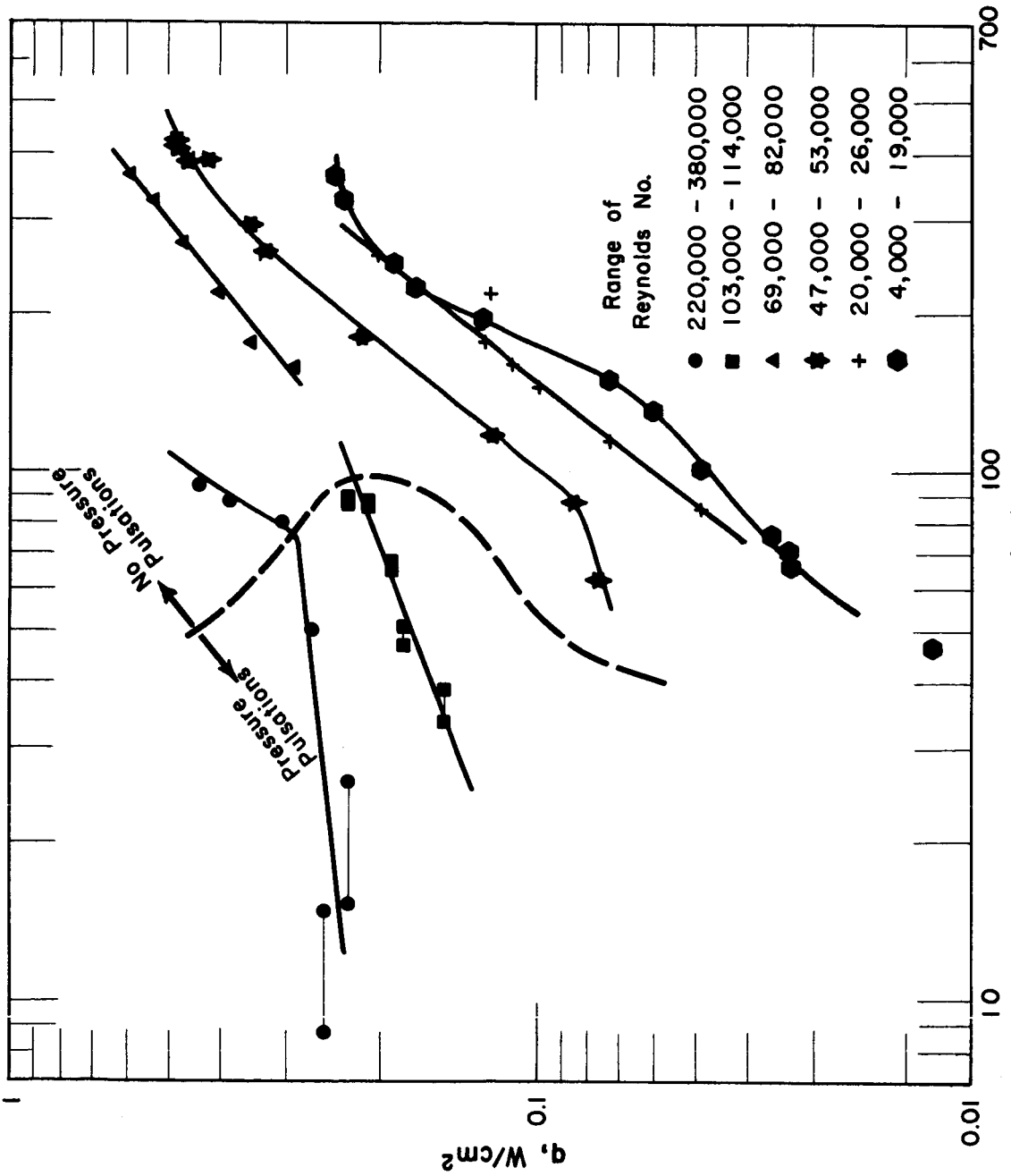


Fig. 8. Heat flux vs temperature difference at station 4. (NITROGEN)

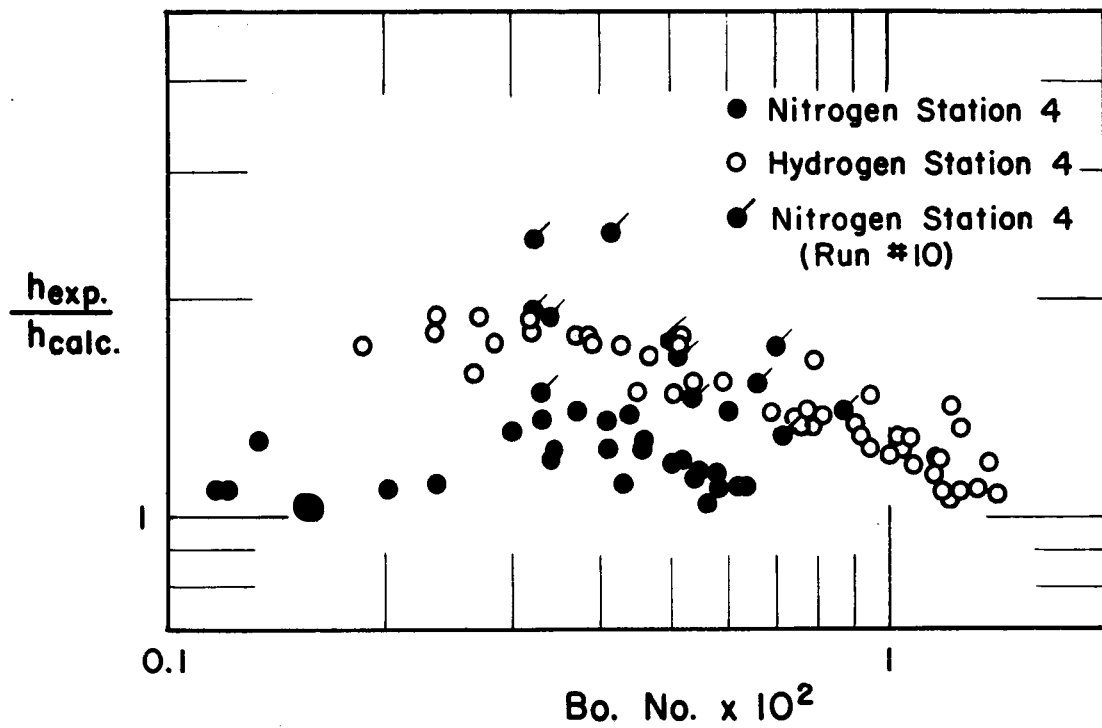


Fig. 9. Heat transfer coefficient ratio vs Boiling number at station 4.
(HYDROGEN AND NITROGEN)

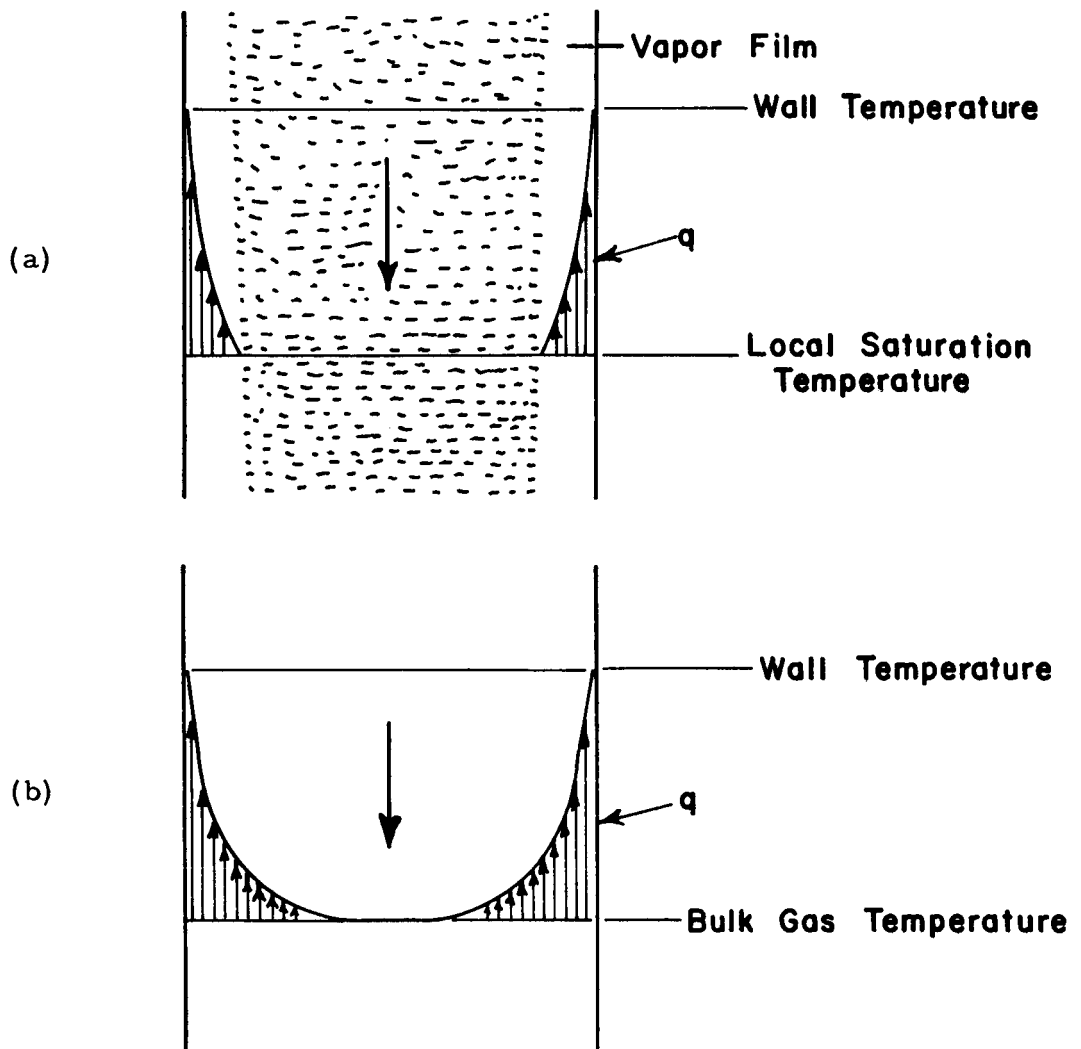


Fig. 10. Illustration of temperature profiles:
 (a) Proposed for two-phase, solid-vapor flow.
 (b) For single-phase, fully developed turbulent flow of a gas.